ROYAL SWEDISH
GEOTECHNICAL INSTITUTE
PROCEEDINGS
No. 8

INFLUENCE OF SAMPLER TYPE AND TESTING METHOD ON SHEAR STRENGTH OF CLAY SAMPLES

By

BERNT JAKOBSON

STOCKHOLM 1954

ROYAL SWEDISH
GEOTECHNICAL INSTITUTE
PROCEEDINGS
No. 8

INFLUENCE OF SAMPLER TYPE AND TESTING METHOD ON SHEAR STRENGTH OF CLAY SAMPLES

By

BERNT JAKOBSON

STOCKHOLM 1954

Ivar Hæggströms Boktryckeri AB.
Stockholm 1955

Contents

Preface

The investigation described in this report was made under the direction of Mr B. Jakobson by the Research Department of the undersigned Institute. The samplers used for this investigation (except the Swedish State Railways sampler and the early piston sampler) were designed and constructed by the Mechanical Department of the Institute.

The report was prepared by Mr Jakobson. § 2 is an abstract of a report by Dr. O. Kulling, State Geologist, who has kindly made a geological examination of one of the cores taken by means of the sampler with metal foils.

Stockholm, September, 1954

ROYAL SWEDISH GEOTECHNICAL INSTITUTE

§ 1. Introduction.

Since its start in 1944 the Swedish Geotechnical Institute has developed soil samplers. In this report we shall deal only with samplers taking undisturbed samples, mainly in clay.

There are two main groups of such samplers. One comprises samplers with a continuously controlled recovery ratio, *i. e.* the samplers with a stationary piston and the sampler with metal foils (1)[1]. The other comprises samplers without this control, *i. e.* open samplers and samplers with a free or a retracted piston.

The behaviour of open samplers in respect of the quality of samples has been extensively investigated by Hvorslev (2). In Sweden we use piston samplers (with a stationary piston), because the clays in this country are usually very soft, and because we believe that this type disturbs the clay less than other types of samplers. It is not probable that Hvorslev's results are directly applicable to piston samplers. On the contrary, it is probable that a tube sampler and a sampler with a stationary piston behave quite differently in some respects.

The development mentioned above has resulted in several types of samplers with a stationary piston. These types differ from one another in area ratio, edge angle, drive range, drive velocity, and other factors. Most of these types are made in a single or a few specimens, since they serve only as links in the chain of development. The testing of the samplers has so far mostly been confined to their operation, and has only to a small extent dealt with their influence on the shear strength of the samples. In order to investigate this influence in a more detailed manner and especially in order to calibrate our newest type of sampler, the pneumatic sampler, we have now made an extensive comparison of the various types of samplers in respect of shear strength.

This investigation comprised seven types of piston samplers designed and constructed by the Institute. Furthermore, the newest type of the Swedish State Railways sampler and the sampler with metal foils were included. These types are briefly described in § 4. They will be described more detailed in a following number of the Proceedings of the Institute.

Samples were taken from different depths by means of all these samplers, and were then tested so as to determine their shear strength and other properties. As there are several methods for determining the shear strength, which often give different results, and as it is uncertain which of them is the most reliable, each sample was tested according to several methods.

[1] Numbers in parentheses refer to the bibliography at the end of this report.

On the basis of earlier experience it was expected that even a sample taken by means of the best sampler loses part of its shear strength during the sampling process. This error combines with the error inherent in the testing methods. Both these errors are unknown. In order to provide a solid basis for comparison, we extended the investigation so as to include a direct determination of the shear strength of the clay in the ground by means of the vane borer. For this reason, a theoretical comparison of various testing methods was also included in the investigation.

One detail of the sampler should be mentioned in this connection. In some types of clay, especially in coarse-grained (fine-sandy and silty) clay, it may sometimes be difficult to convey the samples to the ground surface in spite of that vacuum which would arise if the sample were lost. For this reason, we designed a special type of sample retainer. An additional function of this retainer is to reduce the disturbance of the samples. In this report we have called it "shutter", as it has also other functions than the retaining of the sample. A sampler with shutter and a sampler without shutter, which are otherwise identical, are regarded as two different types of samplers in what follows.

So far the investigations of samplers with a stationary piston seem to be scanty, and the tests described in this report are probably the first systematical study of this subject. However, these tests, though extensive, are confined to a single site. We intend to continue the tests on other sites with other types of clays, but we shall then investigate only a few types of samplers (only those which have proved to be the best).

§ 2. Brief Geological Description of Site.

The site of the borings is situated in a clay region that is bounded in the west by an esker and in the east by moraine hills and rising bedrock (Fig. 1). The Enköping River runs through the plain, parallel to the esker, and flows into Lake Mälaren, about 7 km to the south. The boring site is situated about 30 m east of the river. The distance to the esker is about 470 m, and to the moraine region about 500 m. The ground surface at the boring site lies only 0.3—0.4 m above the surface of Lake Mälaren (the terrain is leveed).

The soil (Fig. 2)[1] consists of post-glacial clay to a depth of 19 m, and below that of late-glacial, varved clay (except a few thin layers as is mentioned below). The borings reached a depth of about 30 m.

The post-glacial clay has a very vague stratification, and it is therefore difficult to decide whether it has been subjected to slides, but it seems to be undisturbed. The main part of this clay, from the ground surface down to a

[1] The following description of the soil concerns only one of the cores, taken by means of the sampler with metal foils. However, within the small boring area, the soil seems to be very homogeneous horizontally, possibly with the exception of the sand layers, which, perhaps, do not extend throughout this area.

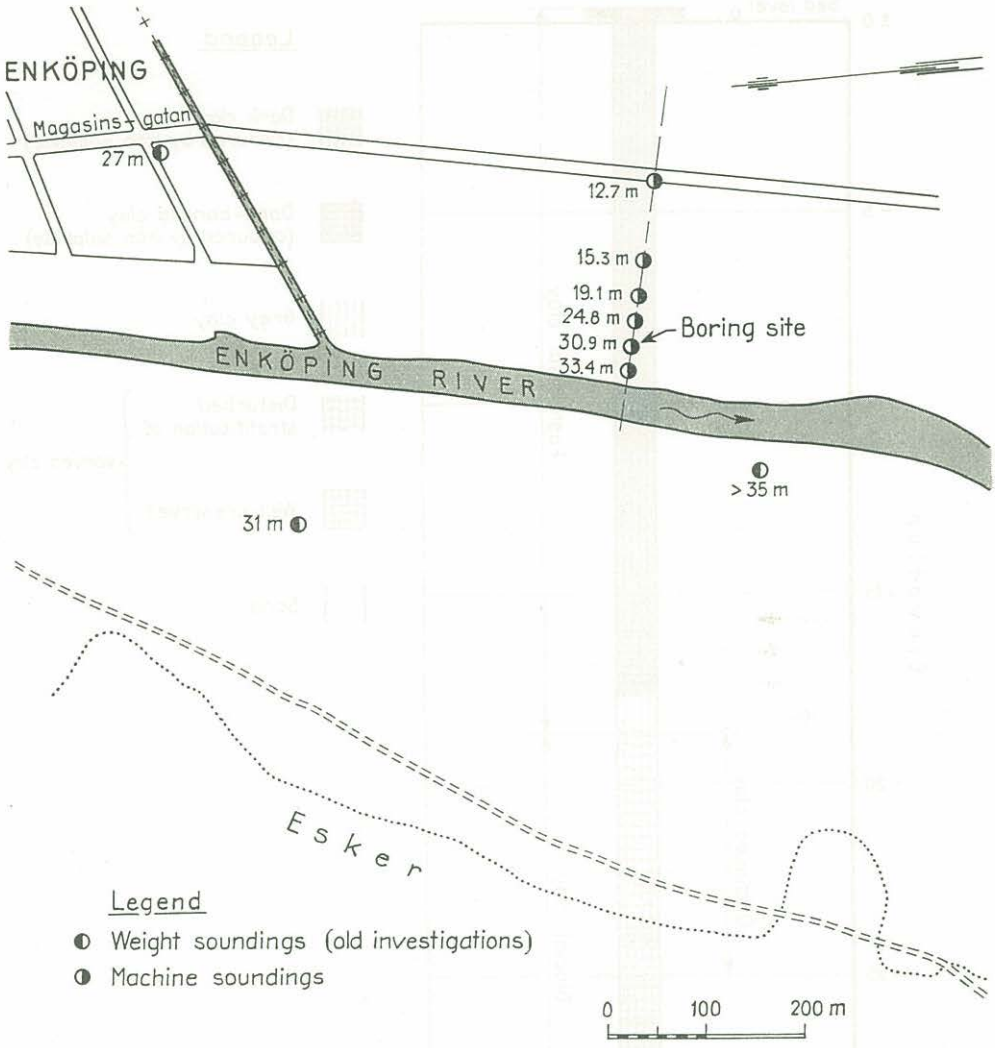

Fig. 1. General plan of site. Depth to firm ground indicated at each bore hole.

depth of 16.2 m, is in a fresh condition greyish black (coloured by sulphide of iron), and has a varying percentage of organic matter. The greatest percentage occurs in the uppermost part of the clay, and at a depth of 10 m (Fig. 16). Next below the dark-coloured clay there is a layer of grey clay, 0.22 m thick, followed by a layer of darker grey clay, 1.44 m thick, with many thin strata blackened by sulphide of iron. Below this, grey clay reappears in a layer 1 m in thickness. Then comes a layer of sand, 0.1 to 0.2 m thick, which separates the post-glacial clay from the late-glacial clay.

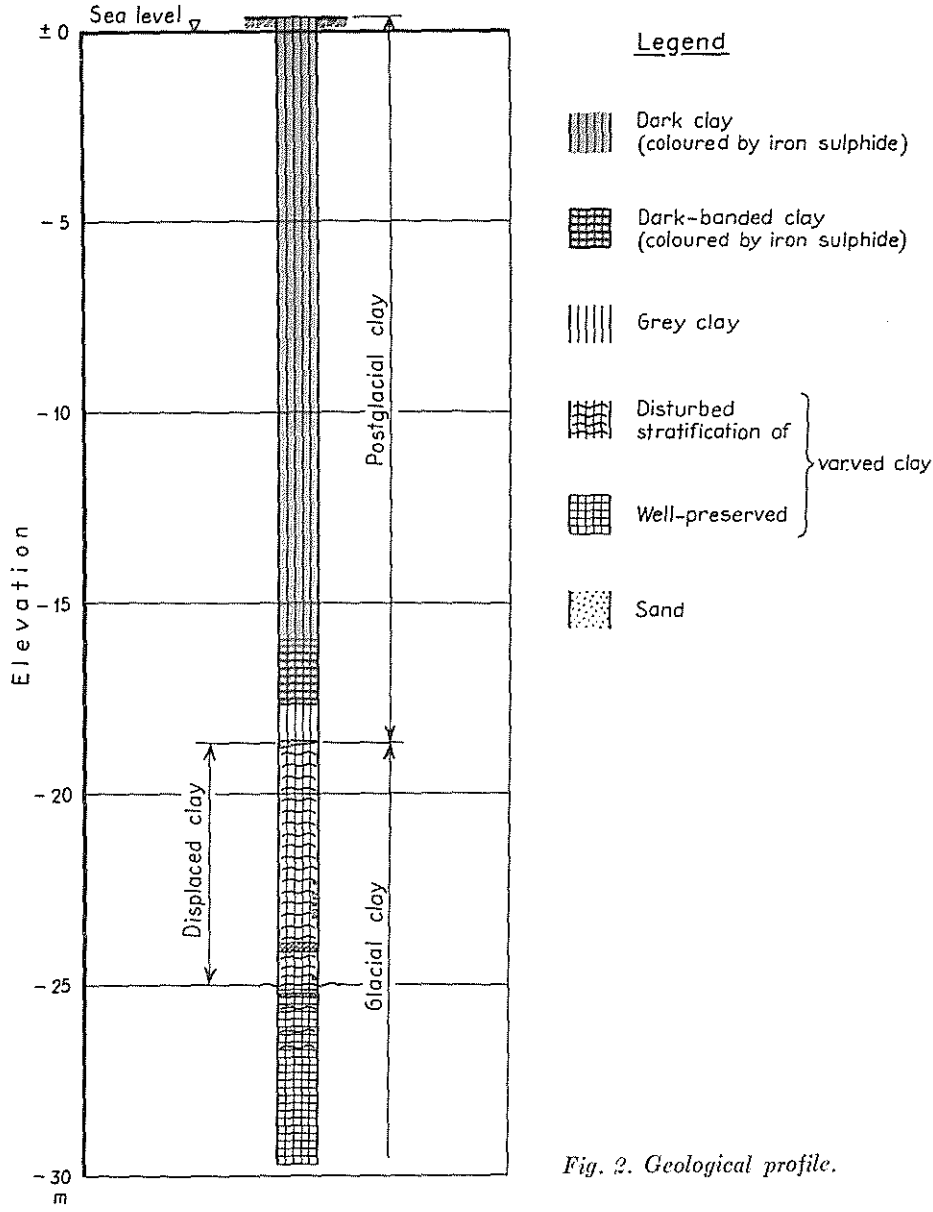

Fig. 2. Geological profile.

In contradistinction to the post-glacial clay the late-glacial, varved clay is severely disturbed in its stratification between 19 and 25 m of depth. It is folded, and contains many old slip surfaces.

Next below this disturbed late-glacial clay comes a layer of grey clay, 0.13 m thick, of the same appearance as the clay directly above the late-glacial clay,

i. e. the post-glacial clay. Below this layer of grey clay there is a layer of clayey sand, not more than 0.03 m thick. Below a depth of 25.54 m the varved clay is undisturbed.

A study of the varve thicknesses shows that a clay mass, several metres in thickness, which has thick varves in its lower part and relatively thin varves in its upper part, has moved over the clay originally deposited on the spot. This above-mentioned clay mass seems to have been brought there either by a slide from the slope of the esker or by a slide from the east, where the depth to the firm ground is considerably smaller than on the boring site. The clayey sand layer next above the displaced clay mass has probably been washed out immediately after the slide.

§ 3. Scope of Tests.

Nine types of samplers were tested. They are described in § 4. A sampler of each type was used to take samples in two diametrically opposed bore holes situated on a circle 4 m in diameter (Fig. 3). Thus, eighteen bore holes at a distance of 70 cm from each other were sunk from this circle.

Owing to this arrangement, all these bore holes are equal in weight, and the variations in the results due to variations in the soil properties may be expected to be equal for all sampler types.

The diameter of the circle was made as small as possible in order to reduce the horizontal variations between the bore holes. However, the distance between

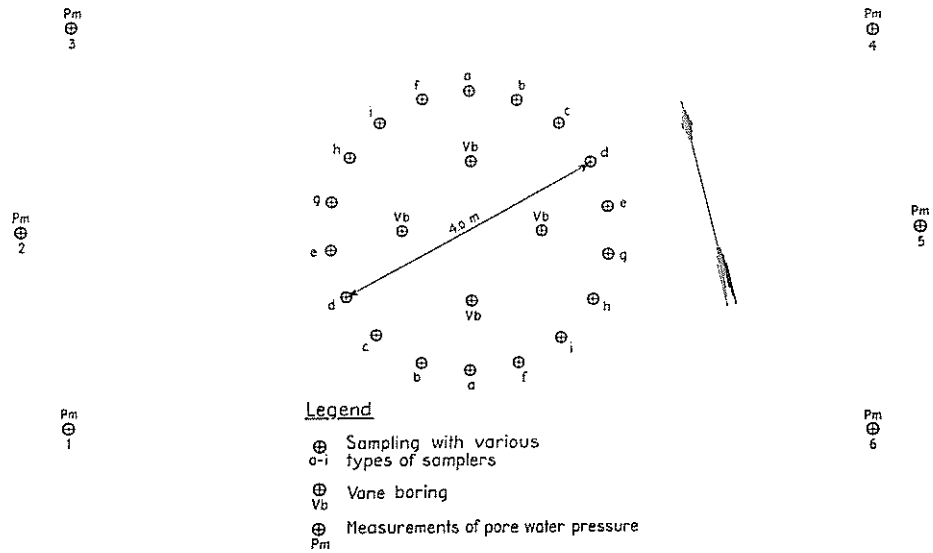

Fig. 3. Plan of bore holes.

the bore holes must be so great that the sampling in one bore hole does not disturb the clay in other bore holes. The results given in § 6 show that the distance between the bore holes was great enough.

In each bore hole a sample was taken at every metre of depth down to a depth of 15 m, and below that at every second metre of depth down to the firm ground. As a rule, the lowest sample was taken from a depth of 29 m. Thus 22 samples were taken from each bore hole, and the total number of samples was 396.

All samples were tested so as to determine the shear strength by different methods described in § 5, the natural water content, the liquid limit, the plastic limit, and the unit weight.

The percentage of organic matter was determined for all samples taken by means of Type *i* sampler[1] (soil sampler with metal foils).

Consolidation tests were made on 16 samples taken at depths varying from 2 to 29 m by means of 3 samplers (Types *c*, *f*, and *g*).

Vane tests were made in four bore holes inside the circle (Fig. 3). They were made at those depths from which samples were taken in the other bore holes, *i. e.* at every metre down to a depth of 15 m, and below that at every second metre. At the same time we also determined the sensitivity of the clay.

Soundings were taken by means of a machine in one section (six bore holes). This machine measures exclusively the point resistance. The maximum driving force of the machine is 1 000 kg. The diameter of the conical drive point can be varied. In this case it was 40 mm. These soundings were taken only in order to determine the position of the firm ground.

Measurements of the pore water pressure in the ground were made in six holes (Fig. 3).

Some of the samples were subjected to differential thermal analyses. Only a few of their results are reproduced in this report.

The results of all above-mentioned investigations are given in § 6.

§ 4. Description of Samplers.

As has been mentioned in § 3, nine types of samplers were used. They are briefly described below.

a. Early piston sampler (without shutter) (Fig. 4) is rather robust. The outer diameter is 83.5 mm, the inner diameter is 60.5 mm, and the range (= L, see Figs 4 to 10) is 250 mm. Thus the area ratio is great, about 0.90. The sampler has no clearance. The sample is obtained in a liner (brass tube) 170 mm in length. This type is the oldest of the Institute's samplers.

[1] Letter symbols designating the types of samplers are given in § 4.

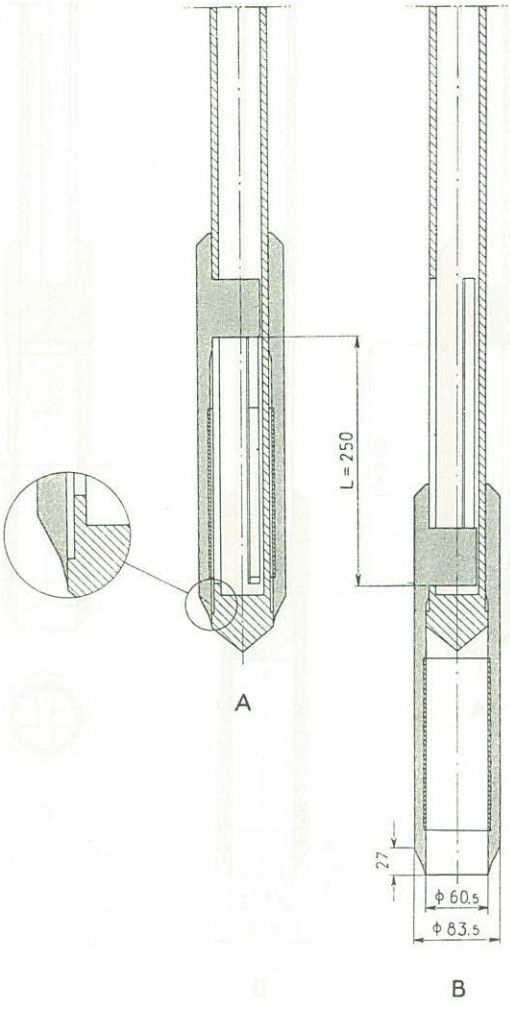

Fig. 4. Schematic drawing of early piston sampler.

b. Early piston sampler with delayed shutter (Fig. 5). The outer diameter has been increased (owing to the shutter) to 88 mm; the inner diameter (60.5 mm) and the range (250 mm) are the same as in Type *a*. Thus the area ratio is still greater than before, about 1.12. The sampler has no clearance, and the sample is obtained in a brass tube as before.

The main purpose of the shutter is to protect the sample during the withdrawal of the sampler. The shutter consists of a cylinder (friction tube) outside the sampler proper, with four steel-strips attached to the lower end of the tube and entering the sampler just above its lower end. During the first phase of

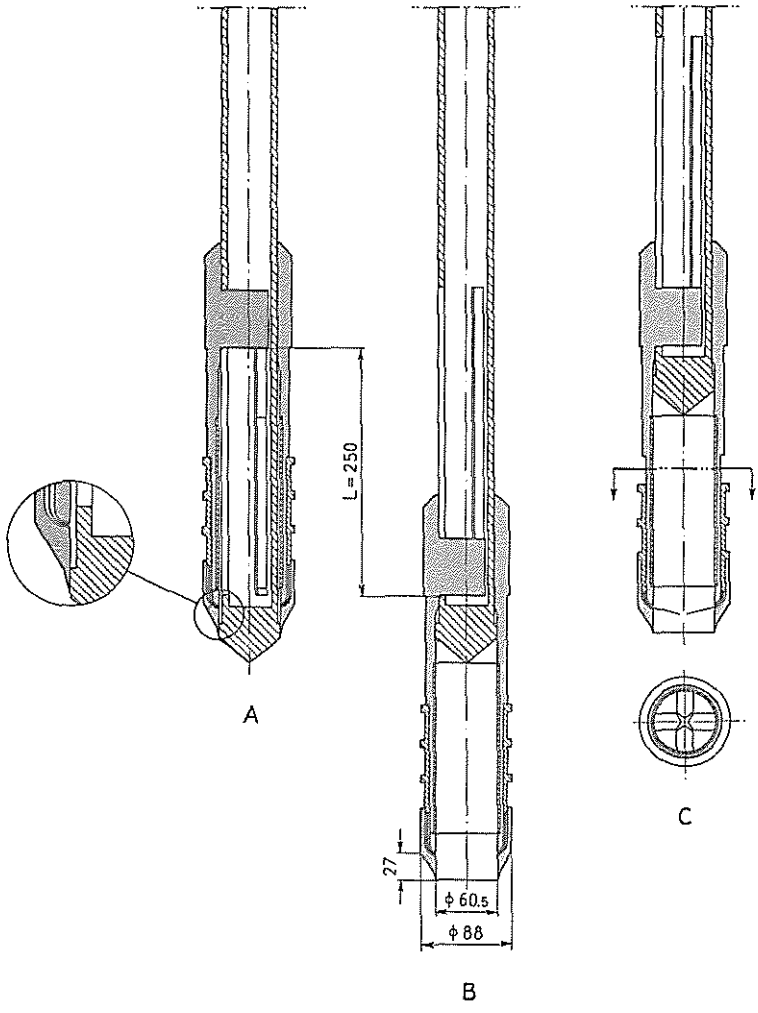

Fig. 5. Schematic drawing of early piston sampler with delayed shutter.

the withdrawal of the sampler the friction tube is kept on a constant level by friction between the tube and the soil. The four steel-strips are therefore forced into the sample a little distance below the brass tube. This occurs gradually during the first centimetres of withdrawal of the sampler (hence the name "delayed shutter").

c. Early piston sampler with instantaneous shutter (Fig. 6). This sampler has the same dimensions as Type *a* (outer diameter, inner diameter, range, clearance), and the sample is obtained in a brass tube in the same way. However, the edge is sharper, and the shutter, fitted with eight

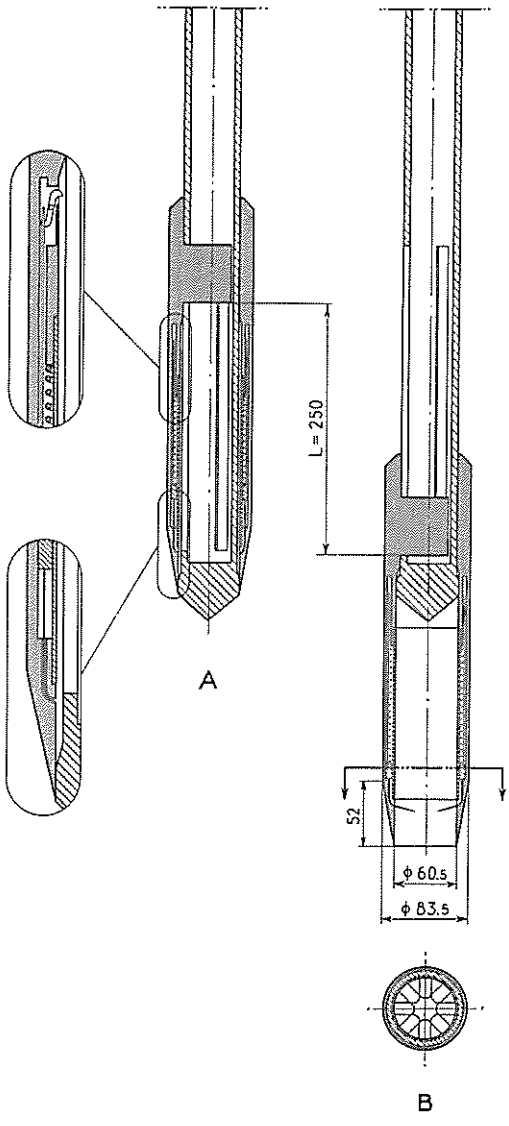

Fig. 6. Schematic drawing of early piston sampler with instantaneous shutter.

steel-strips, is placed in recesses in the lower part of the sampler wall. The shutter is instantaneously operated by a spring as soon as the sampler cylinder reaches its lowest position.

We hoped that the instantaneous cutting of the sample would give better samples than the sampler with the delayed shutter.

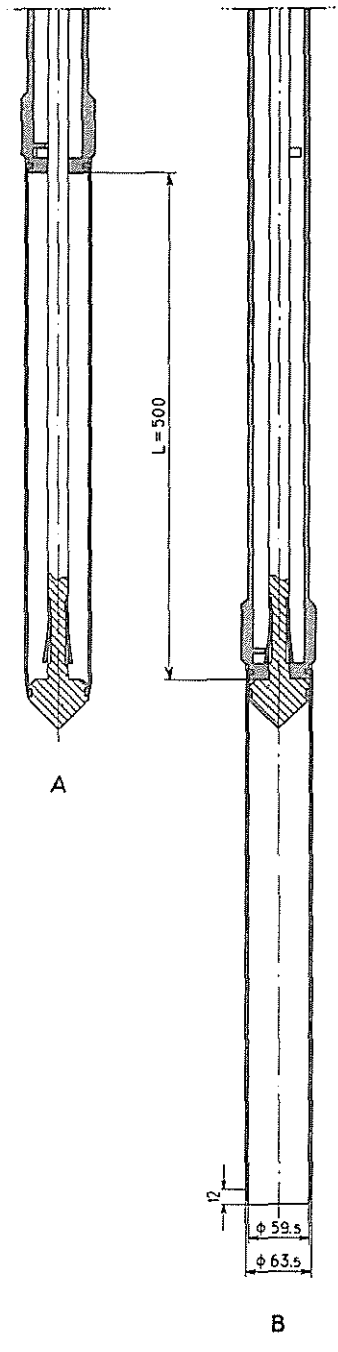

Fig. 7. Schematic drawing of Shelby tube piston sampler.

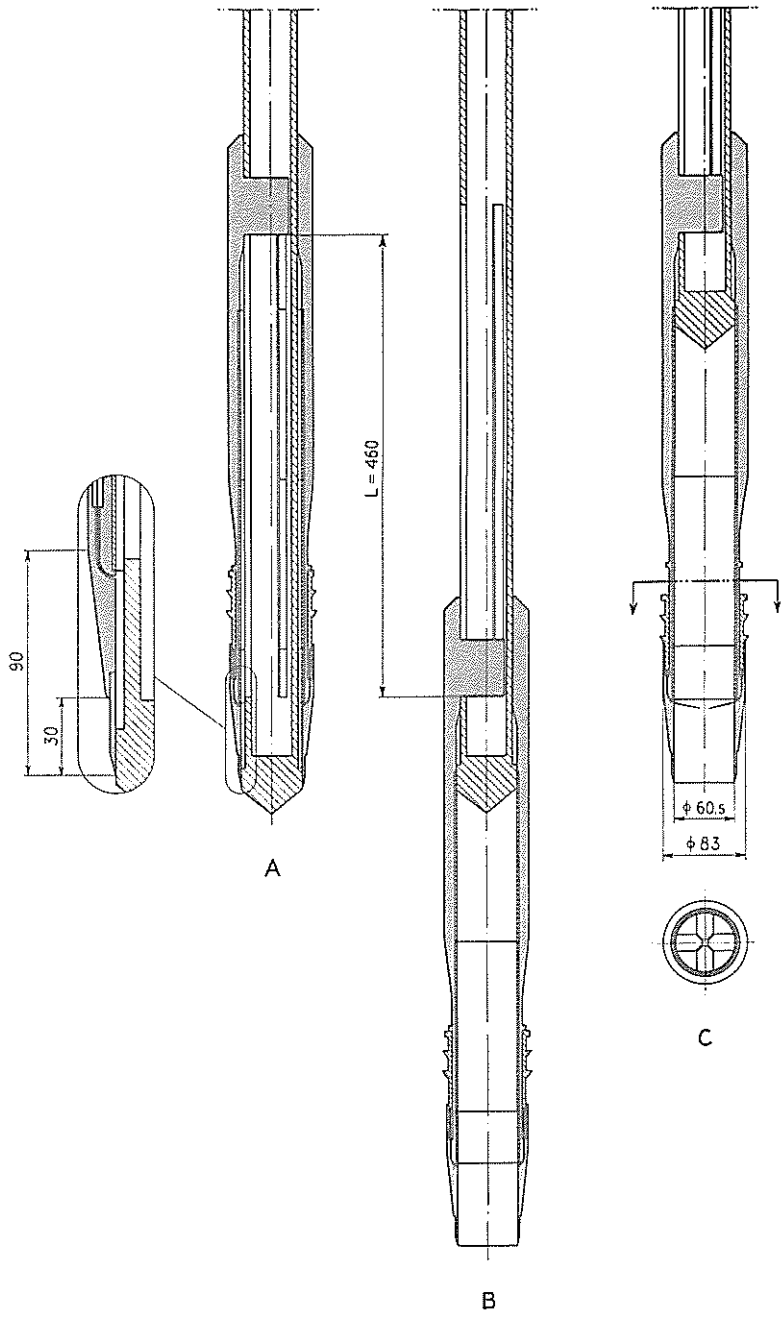

Fig. 8. Schematic drawing of lengthened piston sampler with delayed shutter.

d. Shelby tube piston sampler (Fig. 7). This type was chosen in order to investigate the influence of the area ratio. The outer diameter is 63.5 mm and the inner diameter is 59.5 mm, so that the wall thickness is only 2.0 mm, and the area ratio is 0.14. The range is 500 mm, and the sampler has no clearance. While the sampler is driven into the ground the piston is kept in position by a catch. By turning the piston half a turn the sampler is then released. The sample is obtained directly in the tube, and the whole tube is sent to the laboratory after capping its ends. We used the part of the sample between 25 cm and about 8 cm from its lower end.

e. Lengthened piston sampler with delayed shutter (Fig. 8). This type was designed so as to comply with Hvorslev's requirement that the length of the sample should be great in relation to its diameter. The outer diameter of the lower part of the sampler is 83 mm and the inner diameter is 60.5 mm. Thus the dimensions and the area ratio are very nearly the same as in Types *a* and *c*. However, the edge angle is smaller. The range is 460 mm, and the clearance[1] is 0.5 mm. The sample is obtained in three tubes (liners). The two upper tubes are of normal length (170 mm), while the lowest tube is shorter (58.5 mm). Usually only the part of the sample in the intermediate tube is used, and this was also the case in the present investigation. The shutter is similar in design to that in Type *b*.

f. Pneumatic piston sampler (except for the shutter, this type is quite the same as Type *g*, so Fig. 9 may be used to illustrate this type, too). This type is operated by means of compressed air in order to ensure a rapid continuous drive, as recommended by Hvorslev. The outer diameter of the sampler is 75 mm, the inner diameter is 60.5 mm, and hence the area ratio is 0.54. The range is 450 mm, and the clearance is 0.2 mm. The sample is obtained in three tubes (liners). The respective lengths of the upper, the intermediate, and the lowest tube are 255, 170, and 55 mm. We use the part of the sample in the intermediate tube.

g. Pneumatic piston sampler with instantaneous shutter (Fig. 9). In recesses in the sampler wall a shutter is placed, which is similar in design to that of Type *c*, but is operated by compressed air when the sampler cylinder reaches its lowest position. In all other respects this type is quite similar to Type *f* (equal dimensions).

h. Swedish State Railways piston sampler (Fig. 10). The outer diameter is 55 mm, the inner diameter is 42.5 mm and hence the area ratio is 0.68. The range is 828 mm, and there is no clearance. The sample is obtained in seven brass tubes, 100 mm in length each. According to recommendations, we have used the part of the sample in the lowest tube and in that next above.

---

[1] In Proceedings No. 1 of the Institute (1) it is shown that the clearance is of no use in piston samplers. We had not yet arrived at this result when Types *e*, *f*, and *g* were designed.

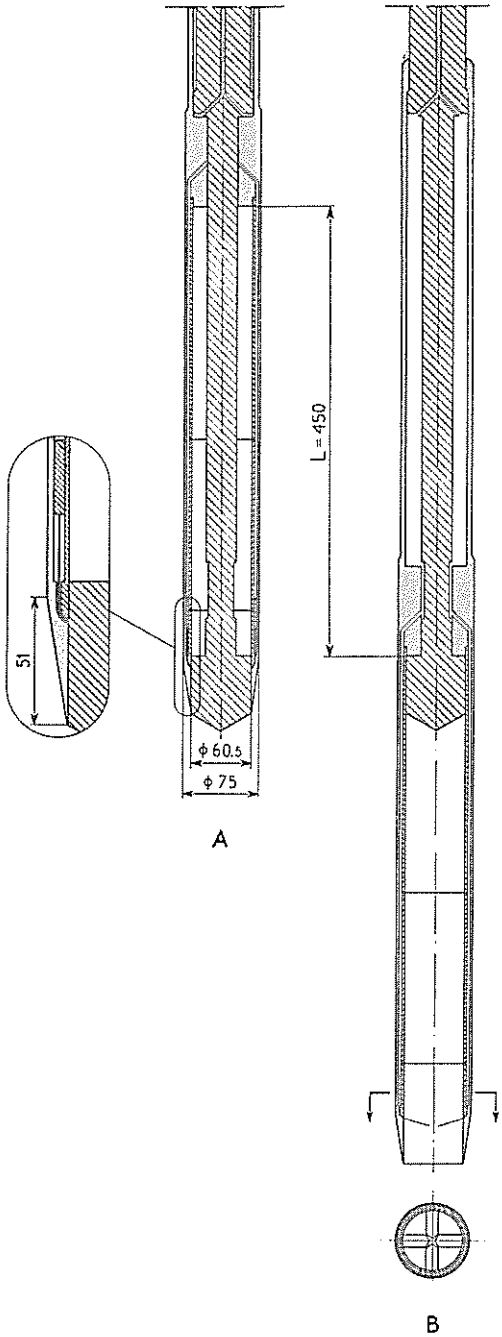

Fig. 9. Schematic drawing of pneumatic piston sampler with instantaneous shutter. Drawn to scale.

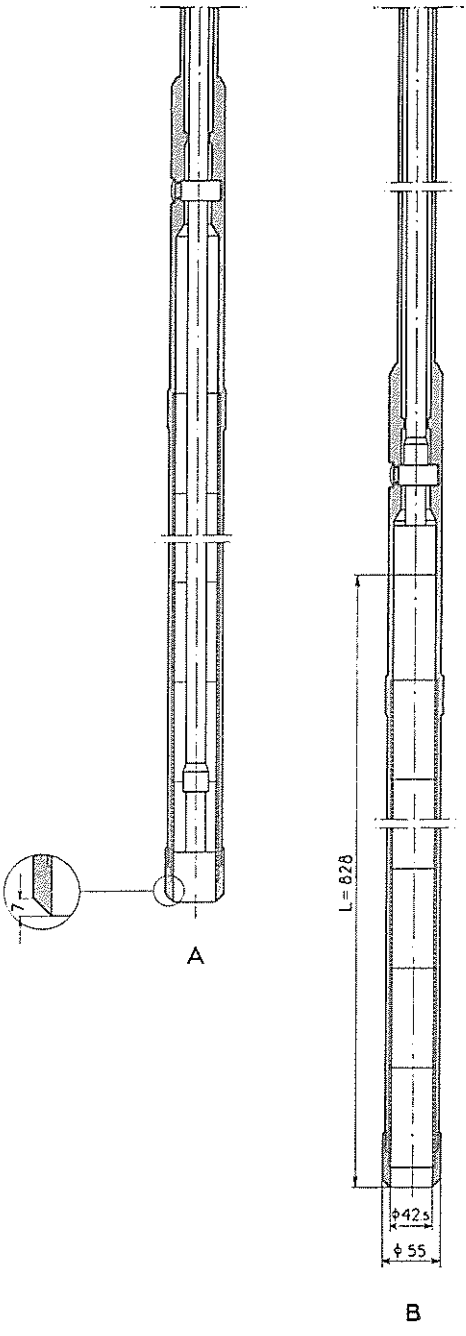

Fig. 10. Schematic drawing of Swedish State Railways piston sampler.

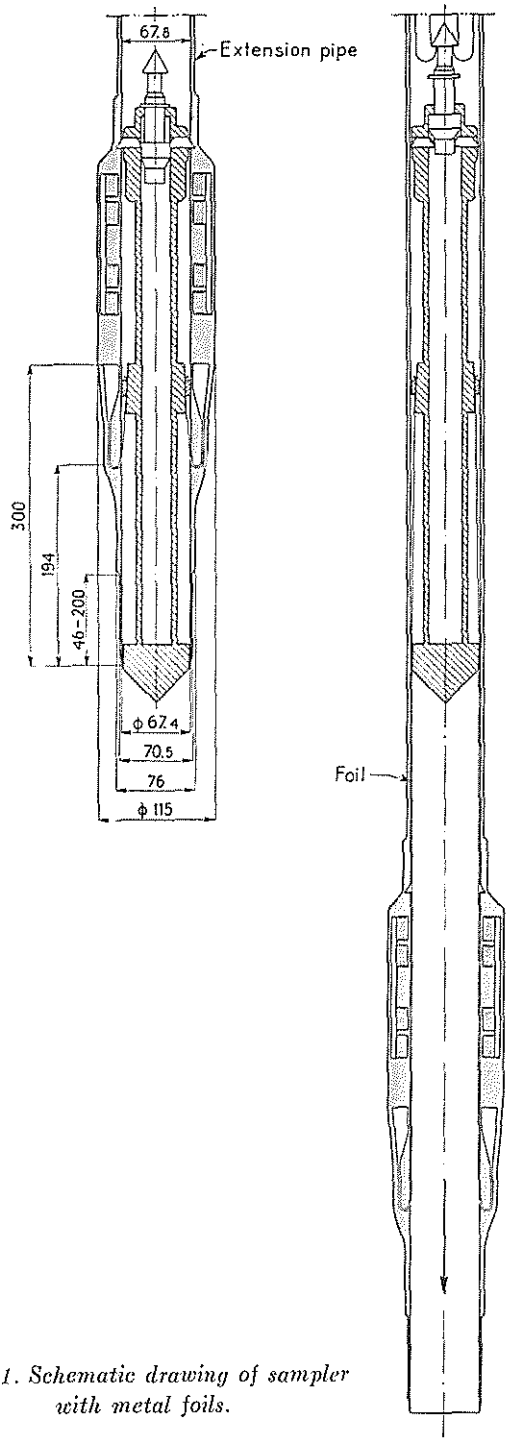

Fig. 11. Schematic drawing of sampler with metal foils.

i. Sampler with metal foils (Fig. 11). The outer diameter of the sampler gradually increases upwards. It is therefore difficult to give any value of the area ratio. The inner diameter is 67.4 mm. The clearance can be varied by using different edges. In this investigation we used no clearance at all. But above the sampling head there is a clearance, as the inner diameter of the extension tube is 67.8 mm. A long, continuous core can be taken in each operation (up to a length of about 20 m or more). Samples, 60.5 mm in diameter, which are adapted to our laboratory equipment, are punched from the core. The sampler is described in detail in Proceedings No. 1 of the Institute (1).

§ 5. Description of Laboratory Testing Methods.

As is generally known, there are many laboratory methods for determining the shear strength of soils, and we had to decide which methods should be used in this case.

As we were interested only in the shear strength of the samples at their original water content, we did not need the triaxial compression test, and we could make the unconfined compression test as well. The direct shear was not used either, because the stress conditions in this test are very intricate, and also because it is time-wasting, and has no special advantages when the water content is kept constant.

Accordingly, partly because of their simplicity, we chose the following tests: the unconfined compression test, the cone test, the laboratory vane test, and, what here is called, the tablet test. These tests are briefly described below.

The unconfined compression test was made in an automatic tester, which graphically records the compression of the specimens as a function of the load (Fig. 12). In the computation of the shear strength we use, as a rule, the original cross-sectional area of the specimen, and not any corrected area, as has been recommended, *e. g.* by Lambe (3). This means that we get somewhat higher values of the shear strength. The shear strength of each sample taken by means of Type *g* (pneumatic piston sampler with instantaneous shutter) was computed by means of both these methods, and the difference between the respective values of the shear strength varied from 3 to 10 %, being on an average 6.8 %.

Note: We should use a corrected cross-sectional area in the computation of the compressive stress and the shear strength, but it is very difficult to say how this correction should be done. Lambe uses the average cross-sectional area, A, found from

$$A = \frac{A_0}{1 - \varepsilon}$$

in which A_0 = the initial cross-sectional area of the specimen and ε = the axial strain. We think that the most correct method would be to use the average cross-sectional area of that part of the specimen in which the surface of failure develops, but it is hardly possible to determine this area. Our most serious objection to the method proposed by Lambe is that after the surface of failure has begun to develop, only a part of the axial strain causes an increase in the cross-sectional area of the specimen.

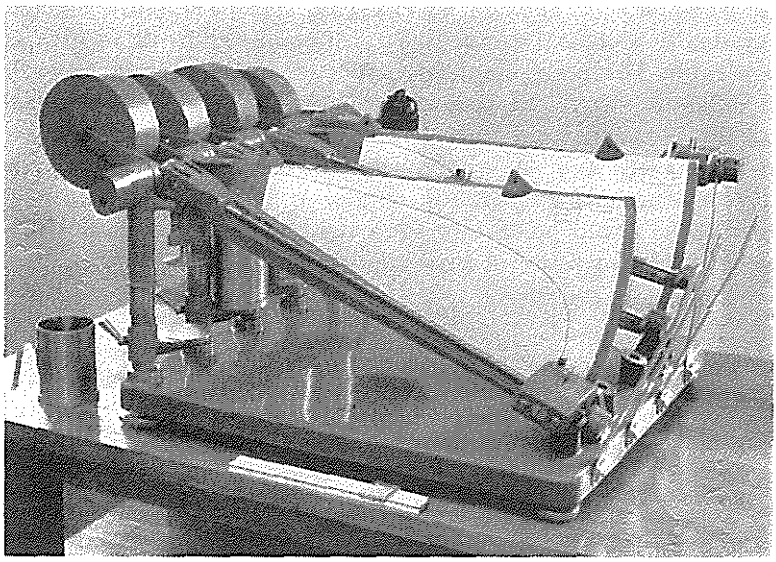

Fig. 12. Automatic unconfined compression tester.

The cone test was made by means of the usual Swedish method. A cone is lowered until its point touches the surface of the clay. Then the cone is released, and sinks by gravity. From the depth of penetration we determine the shear strength by the aid of an empirical law. Normally two cones are used, *viz.*, one having an angle of 60° and weighing 60 g, and the other having an angle of 30° and weighing 100 g.

The laboratory vane test was made in the tester shown in Fig. 13. The vane was 15.3 mm in diameter and 30 mm in height. The sample, kept in the liner, was turned with a velocity of 0.1 degree per sec., *i. e.* the same velocity that we use in the field vane test, and the reaction moment on the vane was measured by means of a torsion pin and mirrors. The trimming of the tester showed that the vane should be lowered until its top was at least 2 cm below the surface of the clay.

The tablet test consists in the application of a test-load to the clay surface by means of a tablet, whose area in this case was only 0.5 cm^2. This test, which is quite new, at least in this country, was made for comparison with the cone test. If we leave out of account the part of the cone below the surface of the clay and the difference in disturbance of the clay between these two tests, then they may be regarded as identical. The shear strength in the tablet test may be put equal to a coefficient (about 0.16) times the normal pressure on the clay surface at failure. The results of the tablet test are not given in this report.

All samples were tested exactly seven days after they had been taken, in

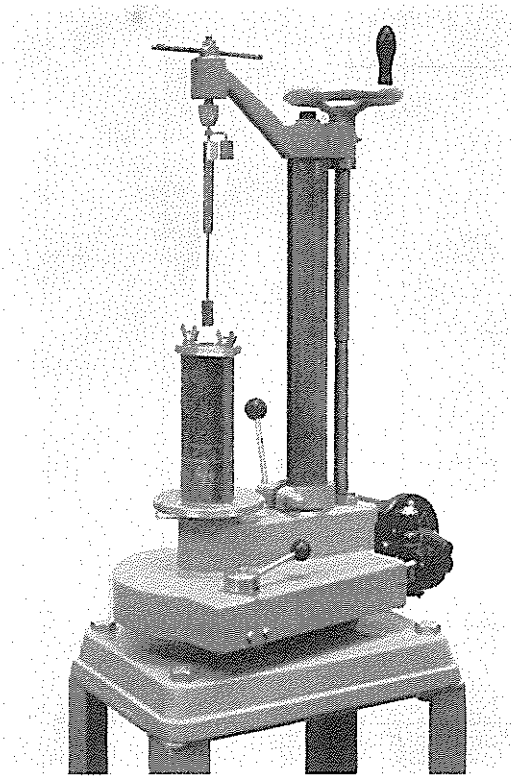

Fig. 13. Laboratory vane tester.

order to avoid any different effects of the time of storage. However, it is not probable that the samples underwent any noticeable change during that time, as they were kept in a humid room in their liners with caps and rubber gaskets.

The shear strength was determined as follows. First, one end of the sample was cut plane. Then the cone test and the tablet test were made on this plane surface three times. After that, the laboratory vane test was made. As has been mentioned above, the vane had to be lowered into the sample to a depth of 2 cm below the surface of the clay. Then about 5.5 cm of the sample was cut away, and three cone tests and three tablet tests were made again, on the new surface. Thus, six cone tests and six tablet tests were made on each sample. We used the mean value of the observations made in these tests. From the remaining part of the sample we cut a piece, as a rule, 10 cm in height, which was used for the unconfined compression test. In some cases a consolidation test was made on the remaining part of the sample. In these cases we used only 8 cm for the unconfined compression test.

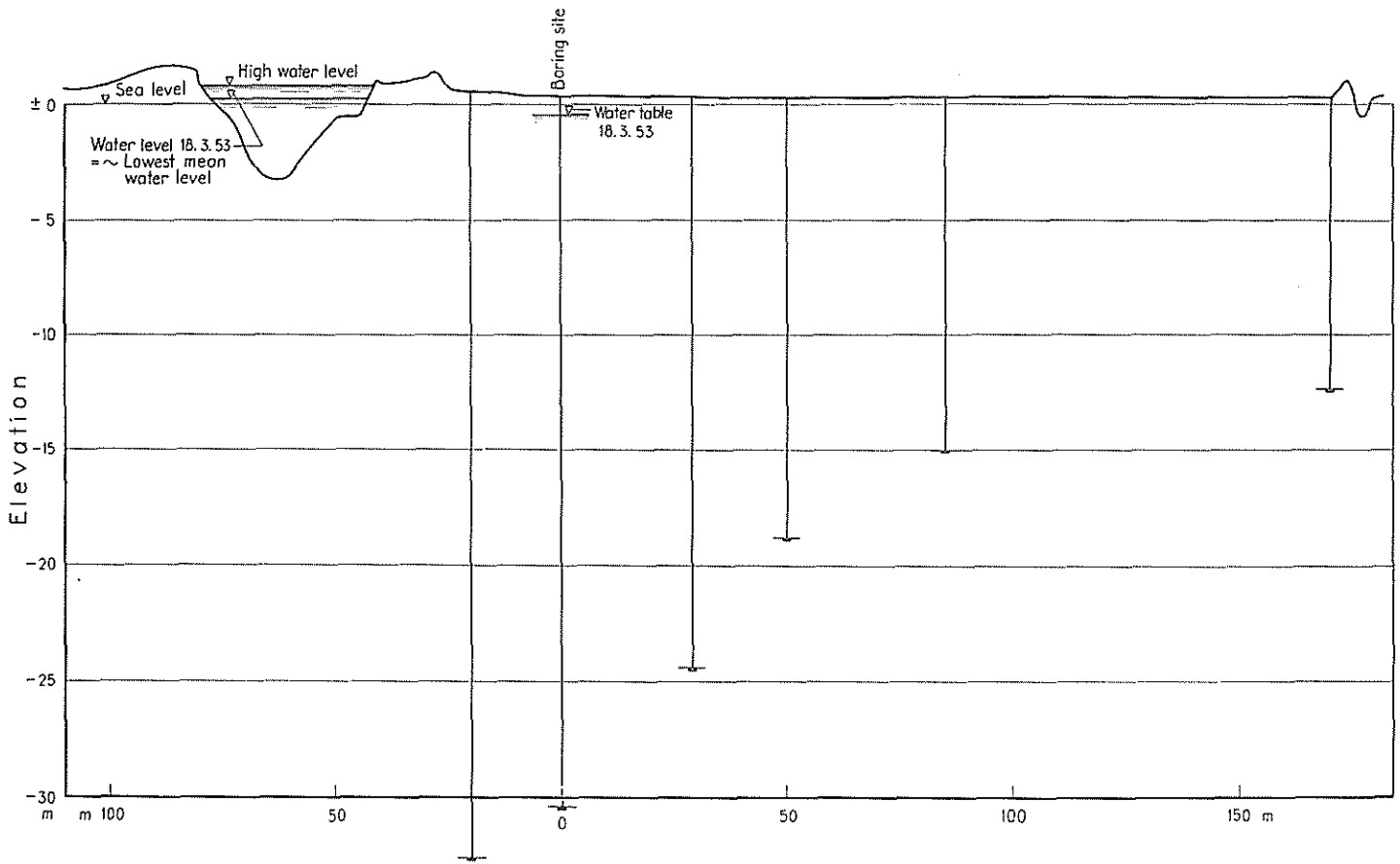

Fig. 14. Results of soundings.

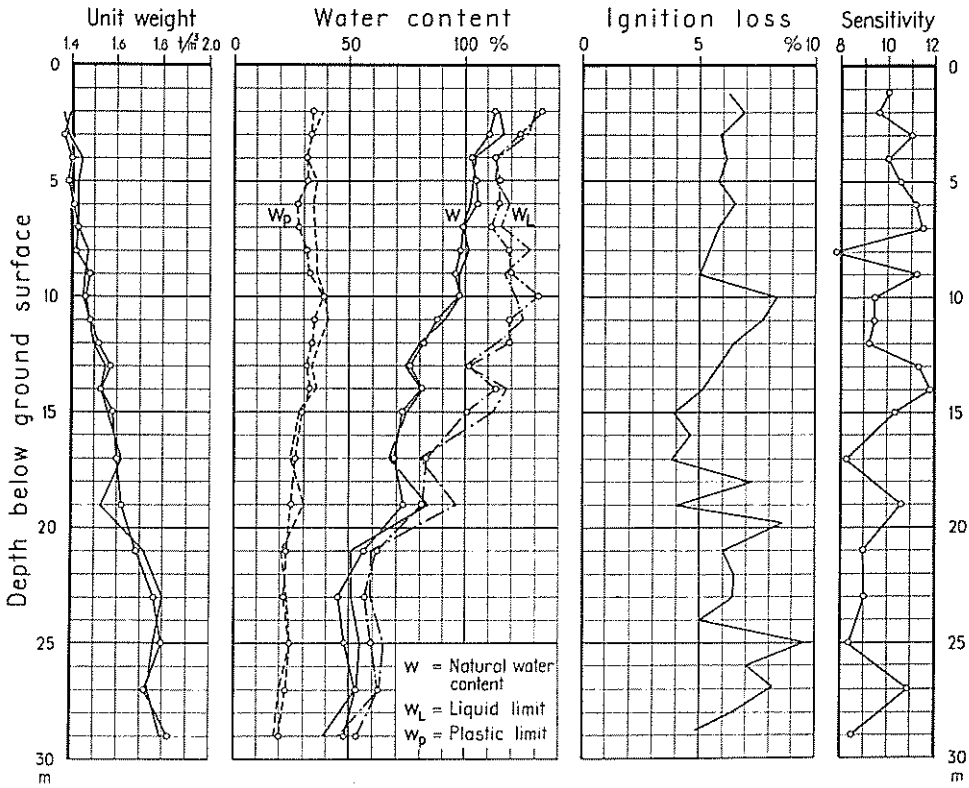

Fig. 15. Standard characteristics of the clay.

As to the other laboratory investigations, there is not much to say. The determination of the unit weight, the natural water content, the plastic limit, and the liquid limit was made as usual, just as the consolidation tests and the differential thermal analyses. The load steps in the consolidation tests were as follows: 0, 0.225, 0.425, 0.825, 1.625, and 3.2 kg/cm^2. On some of the specimens the load was then reduced to 1.625 kg/cm^2.

The percentage of organic matter was determined by measuring the quantity of carbon dioxide after the samples had been calcined. Before that, all carbonate was removed from the samples.

§ 6. Test Results.

The results of the soundings are shown in Fig. 14. The depth to the firm ground is about 30 m on the boring site, but decreases rapidly to the east.

The results of the determination of the unit weight, the natural water content, the plastic limit, and the liquid limit are shown in Fig. 15. However, we have

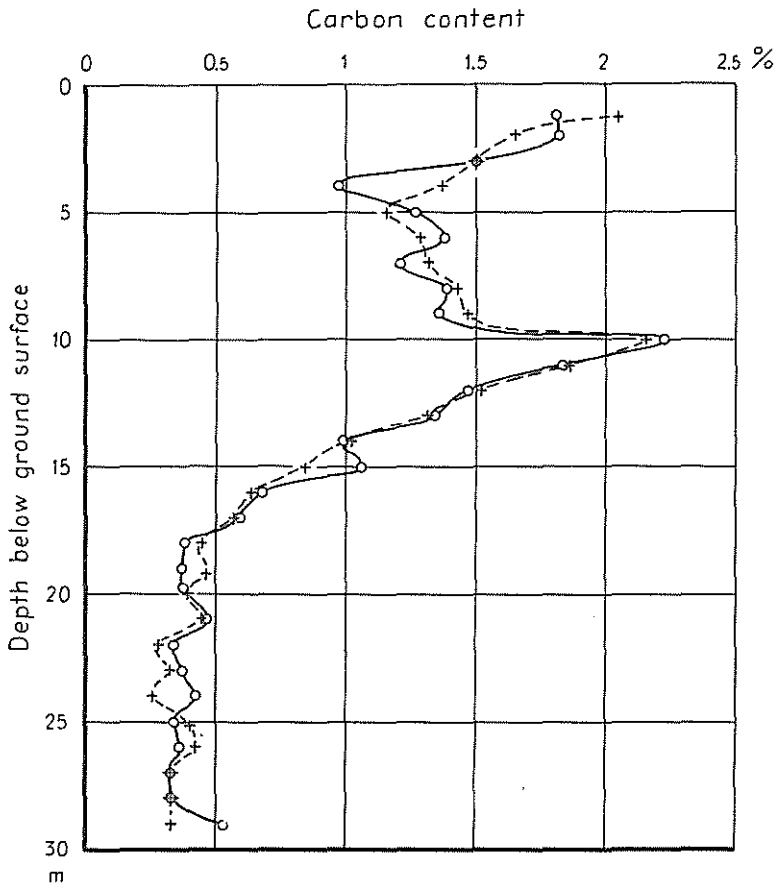

Fig. 16. Organic matter content.

shown only the results relating to the samples taken by means of Type *c* sampler, because the diagrams for different bore holes are very similar. Furthermore, Fig. 15 gives the results of the determination of ignition loss, and the sensitivity (obtained from vane borings). The organic matter content (expressed as pure carbon content) is shown in Fig. 16.

The unit weight increases approximately linearly with the depth. The natural water content decreases on the whole linearly with the depth. The liquid limit is roughly constant (about 120 %) down to a depth of 11 m, then it decreases down to a depth of 21 m, and below that it is constant again (about 60 %). The plastic limit shows the same trend as the liquid limit, but not so evidently, and we can also detect this trend in the carbon content. The ignition loss is high in relation to the carbon content at a great depth, owing to some percentage of lime in the clay at that depth. The sensitivity is normal for Swedish clays (*i. e.* about 10).

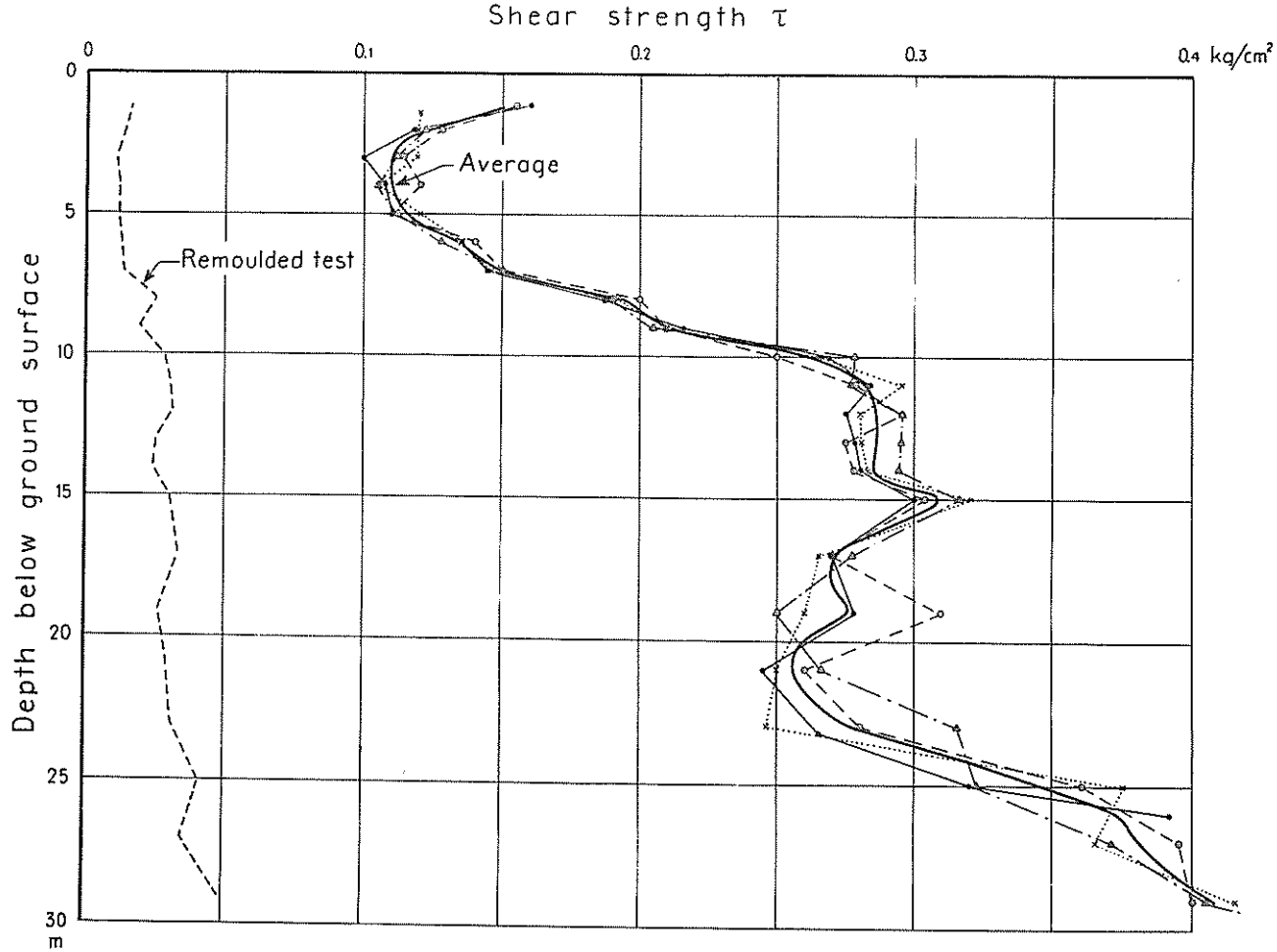

Fig. 17. Results of vane borings.

The results of the vane borings are shown in Fig. 17. The values for the four bore holes agree very well except at the depth where we have found sand layers. The curve of the shear strength as a function of the depth has a very unusual shape. Firstly, the increase of the shear strength in the interval from 5 to 11 m of depth is very great. Secondly, we have the decrease of the shear strength in the interval from 15 to 22 m of depth.

The results of the pore water pressure measurements are shown in Fig. 18. We see that there is an excess pore water pressure in the ground, but it is rather small.

The results of the consolidation tests are shown in Figs. 19 and 20 for five samples only. All consolidation curves are very similar, the compression index being about 1.1. Furthermore, Figs. 19 and 20 also give the vertical effective stress in the ground, which has been computed so as to take account of the pore water pressure measured in the ground. As this stress coincides fairly well with the bend of the curves, we may consider the clay to be normally consolidated.

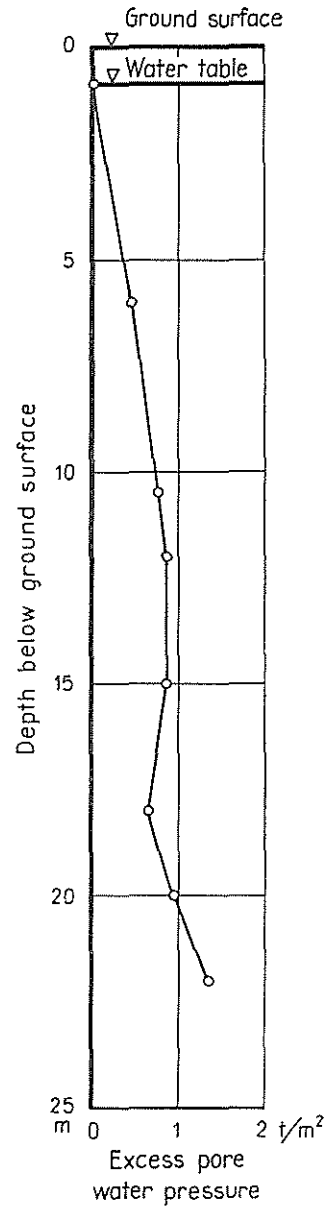

Fig. 18. Results of pore water pressure measurements.

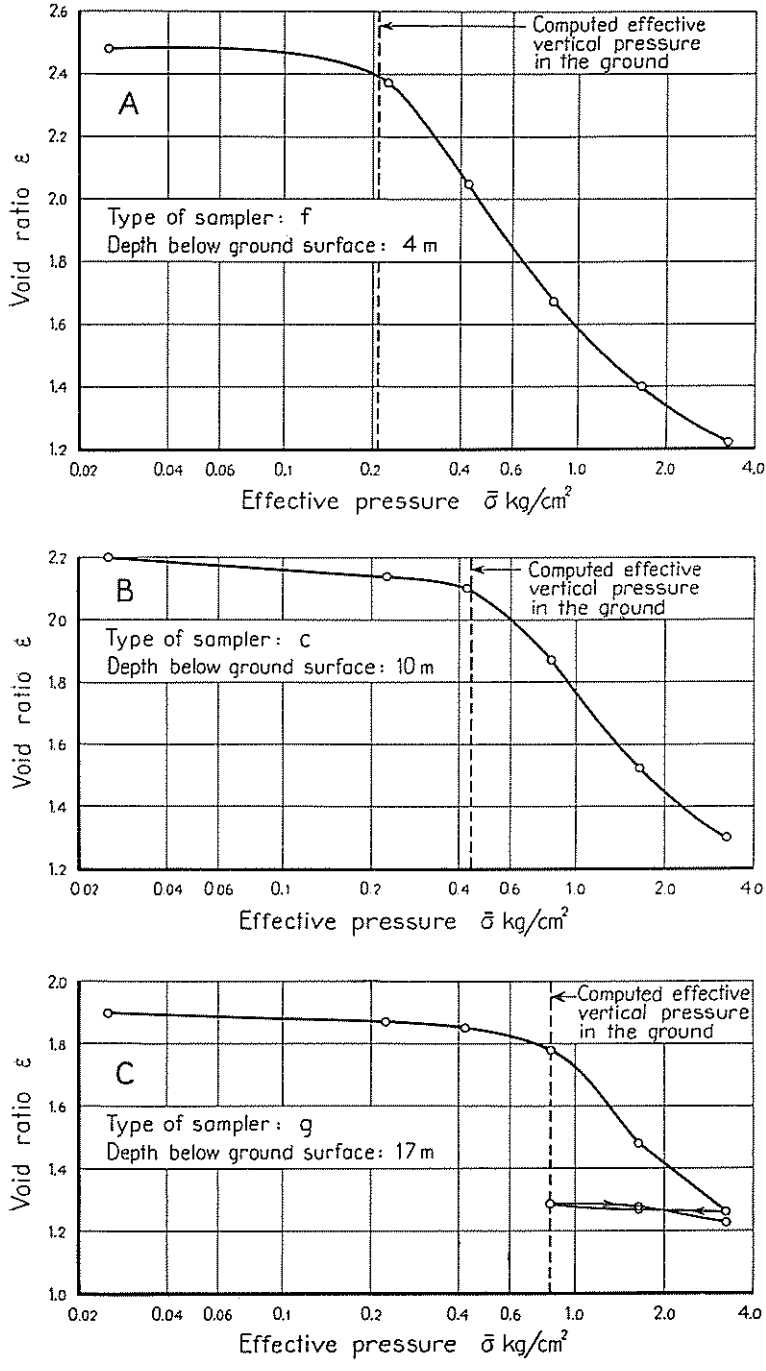

Fig. 19. Results of consolidation tests.

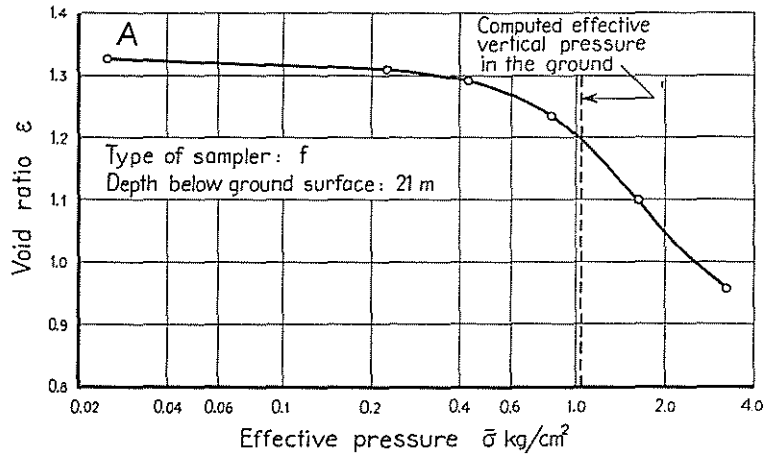

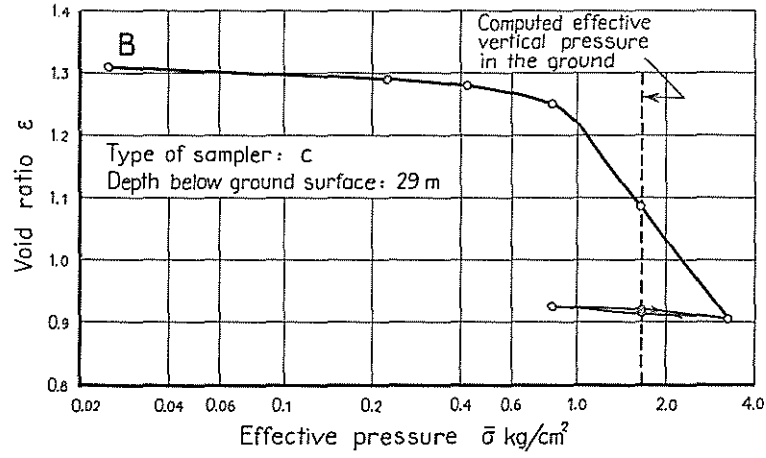

Fig. 20. Results of consolidation tests.

The results of the differential thermal analyses reproduced here are confined to seven samples, see Fig. 21. These curves are rather difficult to interpret. They will be discussed in a following number of the Proceedings of the Institute, together with similar curves obtained on other sites.

The results of the determination of the shear strength by means of laboratory methods are given in per cent of the values obtained from the vane borings. As has been mentioned above, we show only the results of the unconfined compression test, the cone test, and the laboratory vane test. Thus we get three

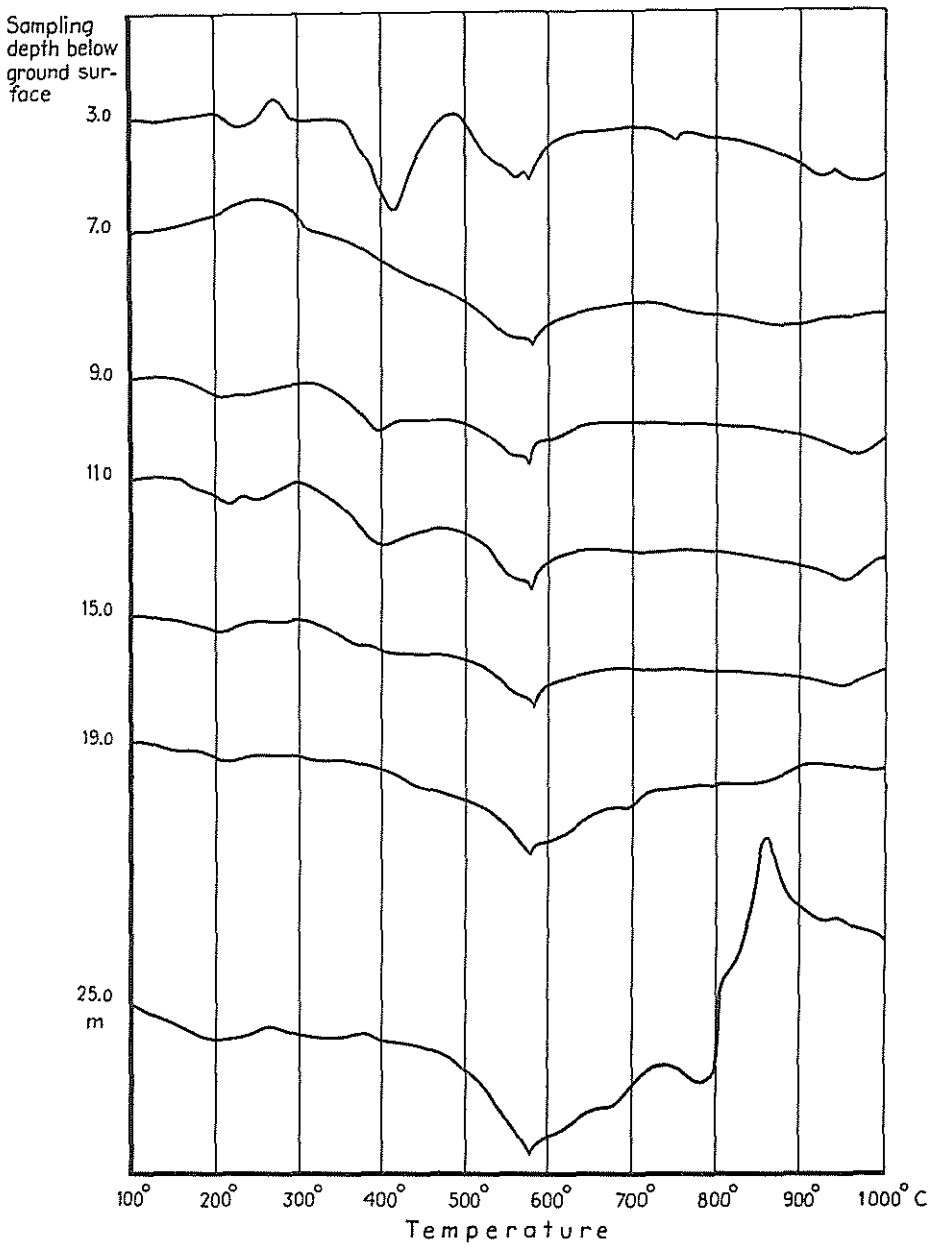

Fig. 21. Results of differential thermal analyses.

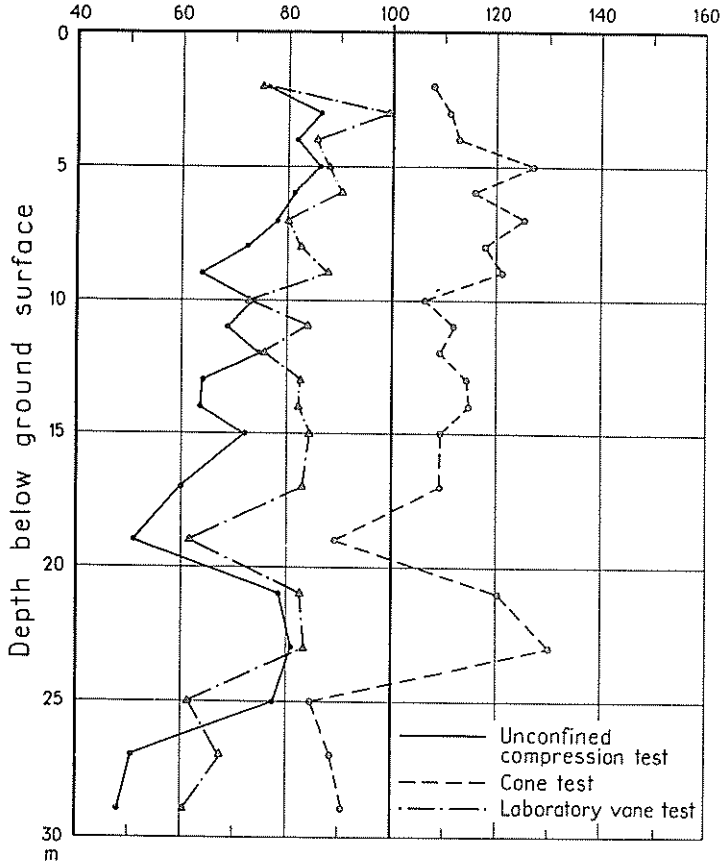

Fig. 22. Ratio of shear strength of samples taken by means of early piston sampler to strength obtained from field vane test.

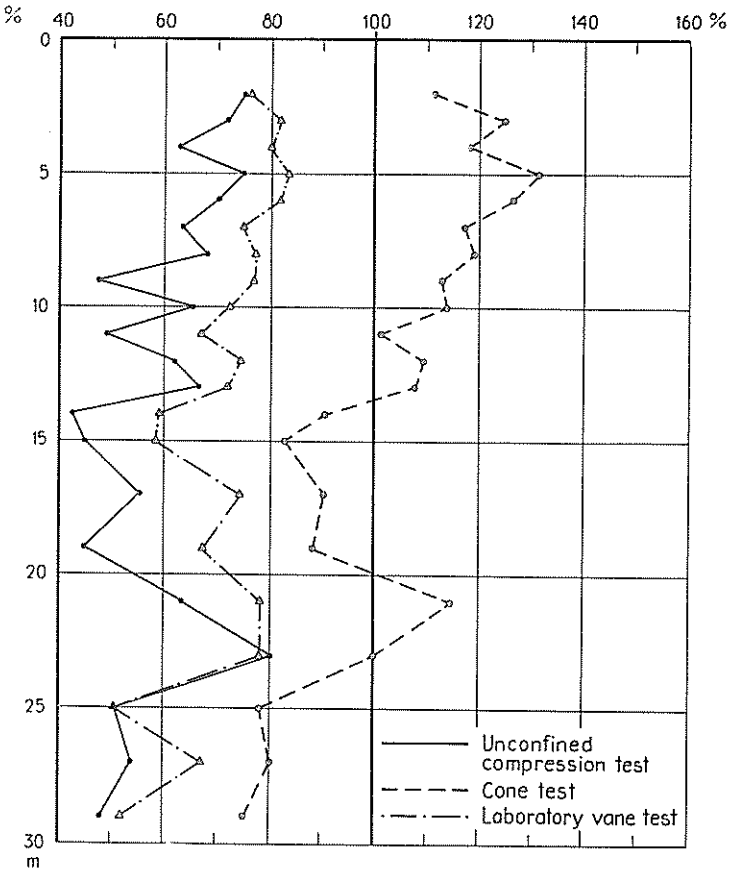

Fig. 23. Ratio of shear strength of samples taken by means of early piston sampler with delayed shutter to strength obtained from field vane test.

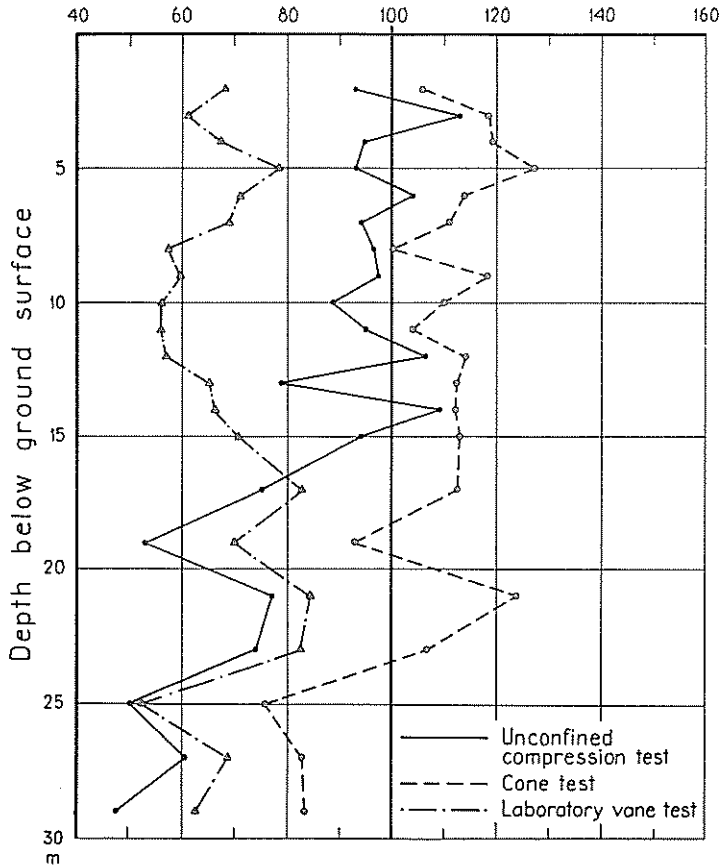

Fig. 24. Ratio of shear strength of samples taken by means of early piston sampler with instantaneous shutter to strength obtained from field vane test.

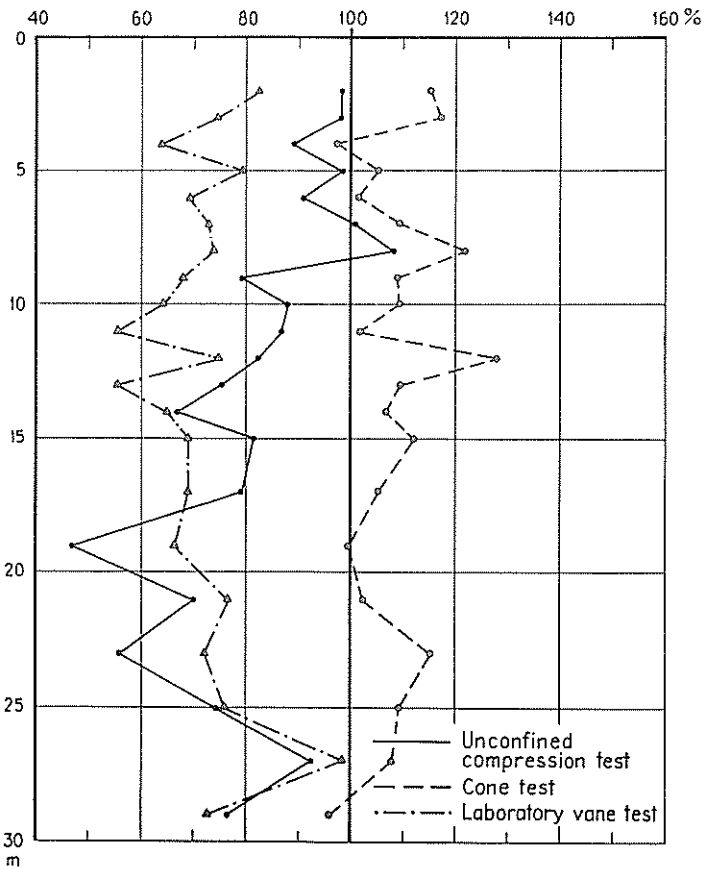

Fig. 25. Ratio of shear strength of samples taken by means of Shelby tube piston sampler to strength obtained from field vane test.

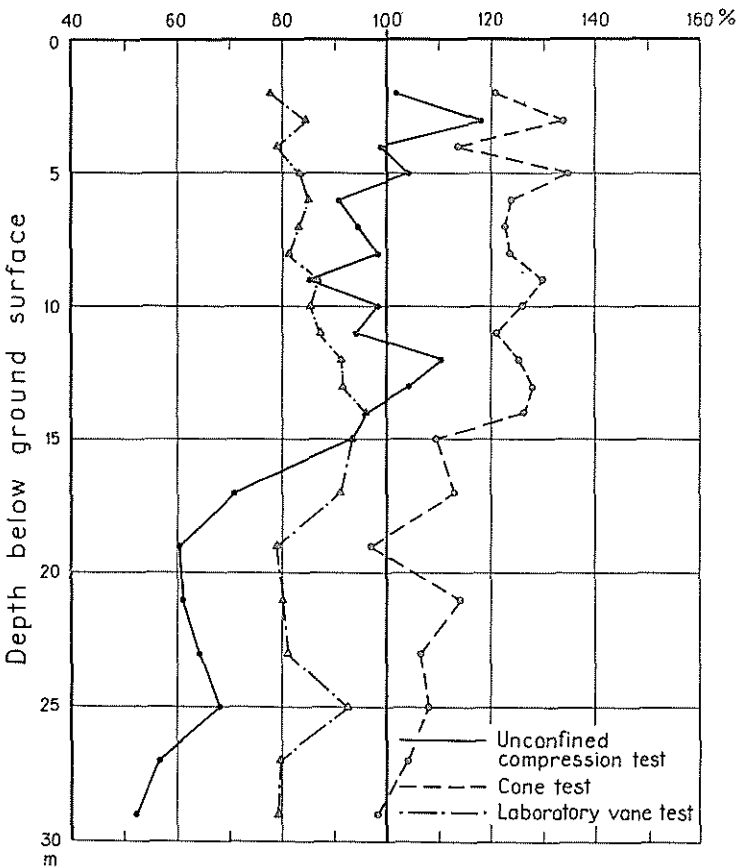

Fig. 26. Ratio of shear strength of samples taken by means of lengthened piston sampler with delayed shutter to strength obtained from field vane test.

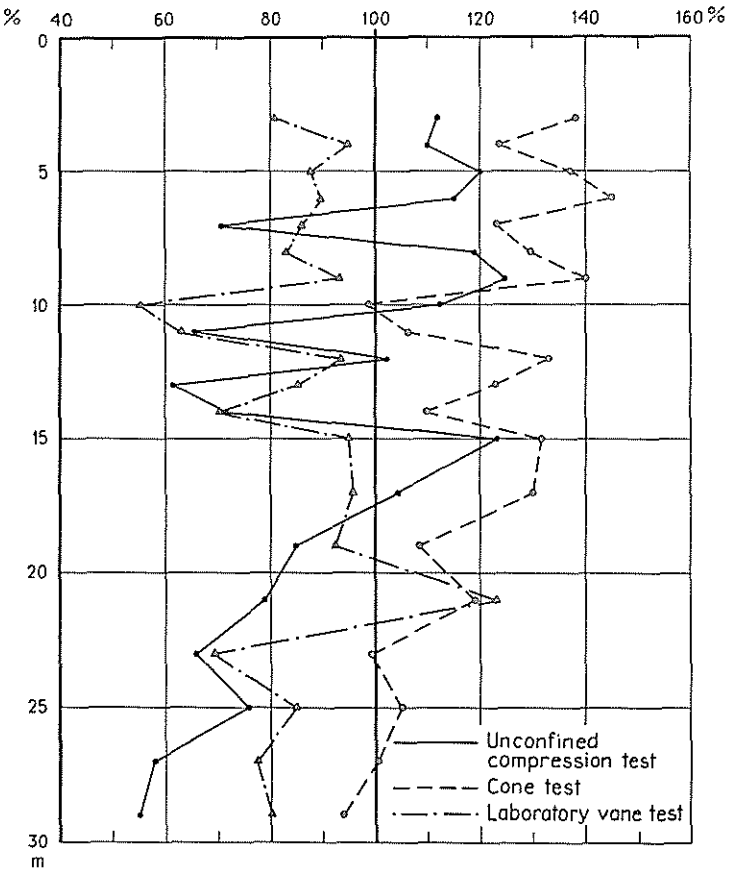

Fig. 27. Ratio of shear strength of samples taken by means of pneumatic piston sampler (without shutter) to strength obtained from field vane test.

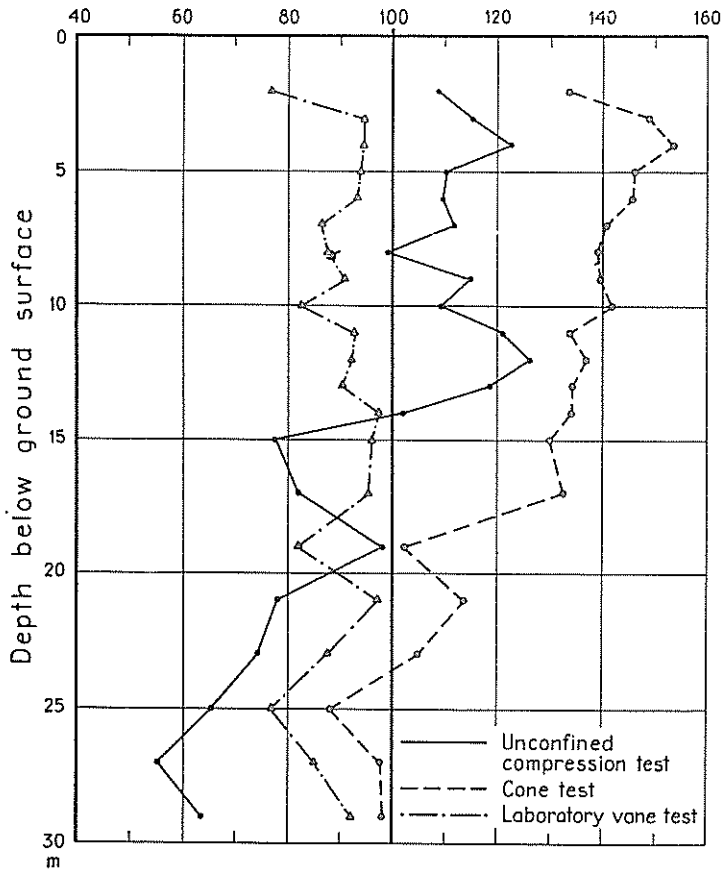

Fig. 28. Ratio of shear strength of samples taken by means of pneumatic piston sampler with instantaneous shutter to strength obtained from field vane test.

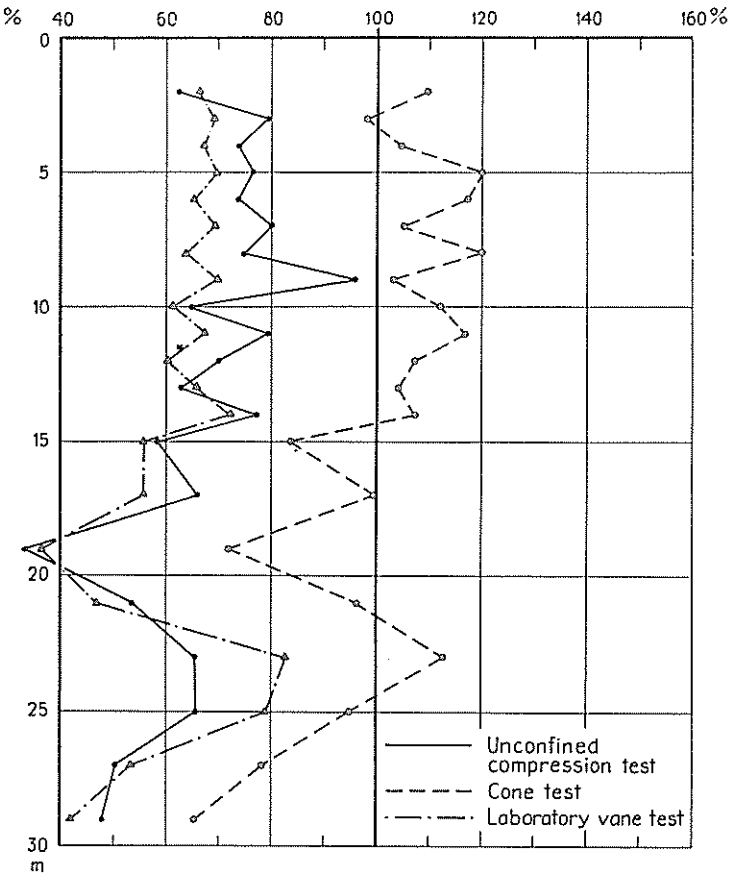

Fig. 29. Ratio of shear strength of samples taken by means of Swedish State Railways piston sampler to strength obtained from field vane test.

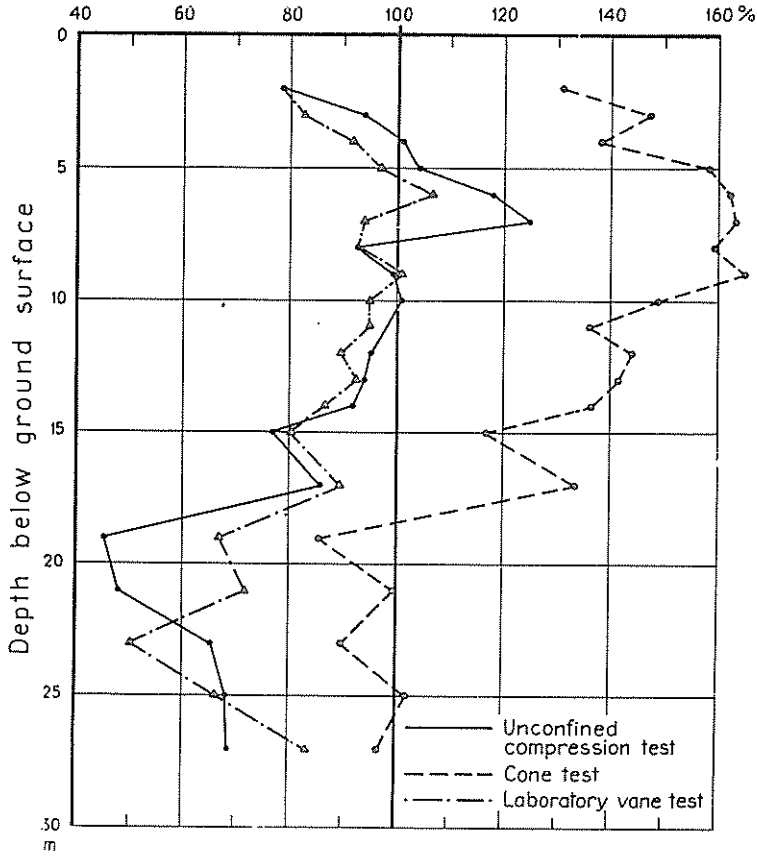

Fig. 30. Ratio of shear strength of samples taken by means of sampler with metal foils to strength obtained from field vane test.

curves for each type of sampler, see Figs. 22 to 30. Each curve is the average of the curves obtained in those two bore holes in which the sampler in question was used.

As a rule, these two curves agree very well, at least as regards the post-glacial clay. As an example we show the two curves for the unconfined compression test on samples taken by means of the pneumatic piston sampler with instantaneous shutter (Fig. 31).

The scattering in the late-glacial clay is quite natural considering the stratification of the clay and in view of the fact that the thin sand layers are not quite horizontal. If the samples were disturbed by the sampling in the adjacent bore holes, it is not probable that these disturbances would be exactly identical in the two diametrically placed bore holes, especially as not all bore holes were

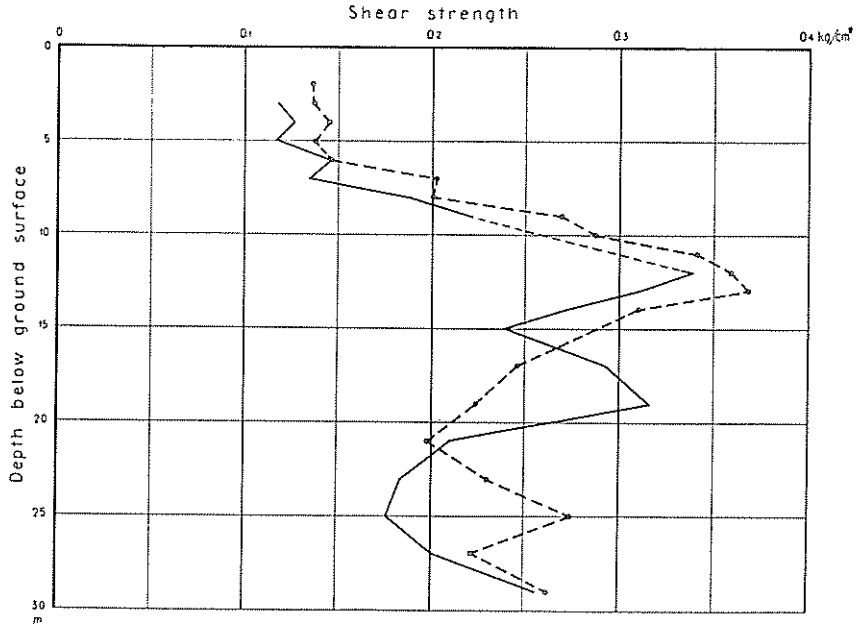

Fig. 31. Shear strength (unconfined compression test) of respective samples taken from two bore holes by means of pneumatic piston sampler with instantaneous shutter.

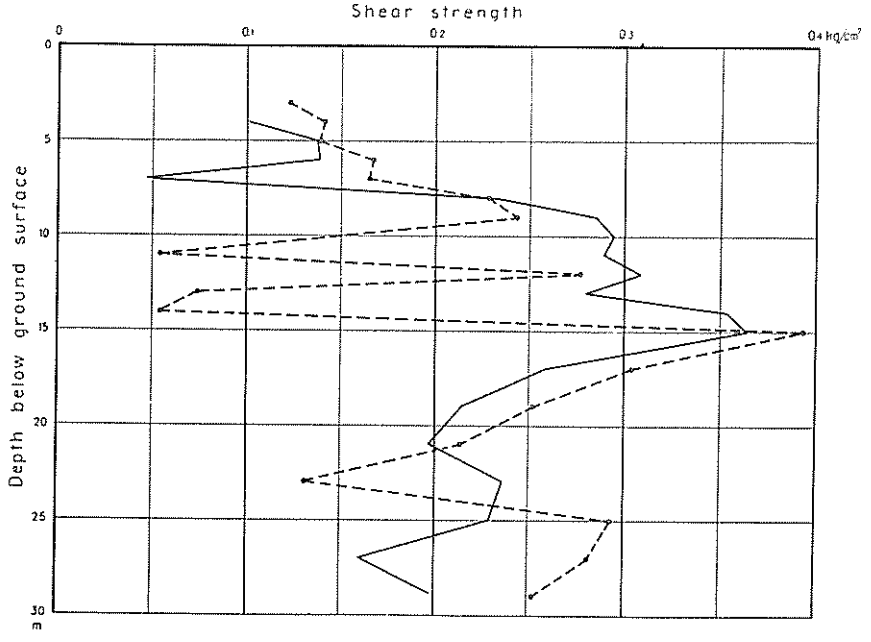

Fig. 32. Shear strength (unconfined compression test) of respective samples taken from two bore holes by means of pneumatic piston sampler without shutter.

used in the same order. Consequently, the close agreement of the two curves may be regarded as a proof showing that the distance between the bore holes was great enough.

However, there is an exception, and that is the result obtained with the pneumatic sampler without shutter (Fig. 32). In this case the difference between the two curves is very great. The most probable reason of this is stated in § 9 a.

As has been mentioned in § 4, we had to punch samples from the core taken by means of the sampler with metal foils, and we used various types of punches. We found that the type of punch had a comparatively great influence on the shear strength of the sample. Fig. 30 shows only the results obtained with our latest type of punch.

§ 7. Discussion of Variation in Shear Strength and in Void Ratio with Depth.

§ 7 a. Variation in Shear Strength.

We have had some difficulties in understanding the unusual form of the curve of the shear strength determined by vane borings as a function of the depth (Fig. 17). The deviation from the normal form could be due to various causes.

In the first place, we could attribute the decrease of the shear strength in the interval from 15 to 22 m of depth to an excessive pore water pressure in this interval. However, Fig. 18 shows that this excessive pore water pressure is so small that it can affect the shear strength only very slightly.

In the second place, we could attribute the great increase of strength in the interval from 5 to 15 m of depth to a preconsolidation of this layer. However, we have found (Figs. 19 and 20) that no preconsolidation can have taken place (except for the superficial layer).

The only remaining cause seems to be some variation in the nature of the clay. The curves of the liquid limit and the percentage of organic matter (Figs. 15 and 16) certainly indicate a variation in the nature of the clay.

There is a correspondence in some respects between the variations in the liquid limit (and the percentage of organic matter) and in the shear strength. When the shear strength increases, *i. e.* in the upper part and the lower part of the curve, the liquid limit is approximately constant, and when the shear strength is constant, *i. e.* in the intermediate part of the curve, the liquid limit decreases.

It is possible but not likely that the corresdondence between the liquid limit and the shear strength can completely explain the unusual form of the shear strength curve. For instance, the increase of the shear strength in the interval from 5 to 11 m of depth is as great as 0.82 times the increase of the normal effective stress, although the liquid limit is constant. For normal clays, at least

normal Swedish clays, the coefficient of increase is 0.3 to 0.4. Accordingly, we believe that there must be some variation in the clay minerals, and this was the reason for our differential thermal analyses. However, as has been mentioned above, we are not yet prepared to discuss these results. Moreover, the question of clay minerals exceeds the scope of this paper[1].

§ 7 b. Variation in Void Ratio.

In Fig. 33 the full-line curve represents the void ratio before the consolidation test (see § 3) of all samples from different depths as a function of the sampling depth. The dash-line curve shows their void ratio after reconsolidation under the computed vertical effective pressure at this depth.

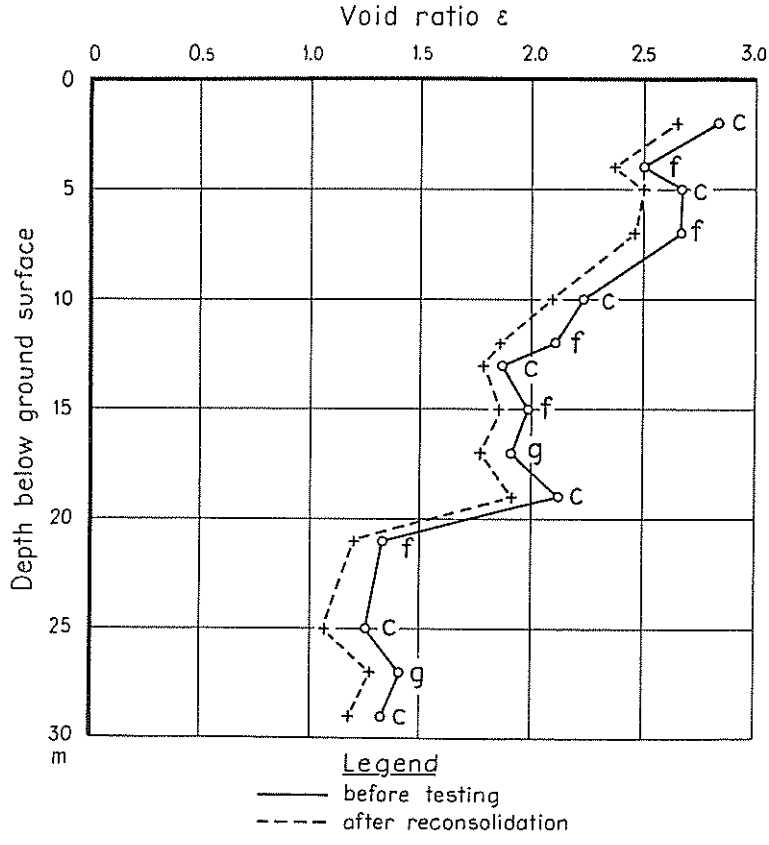

Fig. 33. Void ratio as a function of depth.

[1] Mr I. Th. Rosenqvist, Norway, has suggested that the explanation is a variation in salt content, but a later investigation in this respect showed that this explanation is not correct either.

The close agreement of these two curves is notable. The void ratio of each sample after reconsolidation is somewhat lower than before testing. This slight squeezing-out of pore water from the sample may be due to three causes.

Firstly, each removal and reapplication of load usually produces a slight compression. If we assume that the horizontal effective pressure in the ground is equal to the earth pressure at rest, that the coefficient of earth pressure at rest is 0.5, and that Hooke's law is valid in this case, then the vertical effective pressure during the sampling will decrease from $\bar{\sigma}_v$ to $\frac{2}{3}\,\bar{\sigma}_v$ (we also assume that there is no swelling). In the consolidation test the vertical pressure will increase to $\bar{\sigma}_v$ again.

Secondly, the samples may have been a little disturbed. In that case a reapplication of load always causes a decrease of the void ratio. However, this is probably not a correct explanation in our case, because the decrease of the void ratio seems to be independent of the sampler type and of the depth.

Thirdly, the sum of the principal effective stresses increases[1] during the consolidation test, although the vertical stress is the same as in the ground. The Author does not share the opinion that only the major principal stress influences the void ratio.

However, as has already been mentioned, the difference in void ratio is very little. Therefore, we can state that, in this case, the real effective pressure in the ground cannot be appreciably smaller than its computed value. This is not in agreement with the suggestion made by Terzaghi (4) in 1941.

§ 8. Theoretical Comparison of Field Vane Test, Laboratory Vane Test, and Unconfined Compression Test.

§ 8 a. General.

In order to be able to discuss the results of the shear strength determinations given in § 6, we have to make a theoretical comparison of the various tests. However, the cone test is very difficult to analyse, or even to compare with the other tests, so that we shall confine ourselves to a comparison of the field vane test, the laboratory vane test, and the unconfined compression test.

Notation.

$\bar{\sigma}_v$ = vertical effective stress in the ground
$\bar{\sigma}_h$ = horizontal effective stress in the ground
c = true cohesion in the ground
c_o = origin cohesion[1] in the ground
$\varkappa$ = coefficient of increase in cohesion

[1] This question will not be discussed here.

φ = true angle of friction
$\bar{\sigma}$ = effective normal stress on slip surface
σ = unconfined compressive strength
τ = shear strength
$\tau_c = \frac{\sigma}{2}$ = shear strength from unconfined compression test
τ_v = shear strength from field vane test
τ'_v = shear strength from laboratory vane test
M = maximum torsional moment in vane test
D = diameter of vane
H = height of vane
λ = compressibility ratio
λ_r = recompressibility ratio
τ_{ver} = shear strength in a vertical surface of rupture
τ_{hor} = shear strength in a horizontal surface of rupture
K = coefficient of earth pressure at rest
n = a coefficient $= \frac{1 - \lambda}{1 + \lambda}$

We suppose that the clay is normally consolidated, as has been indicated by our consolidation tests. However, even if the clay should be preconsolidated, we can still use the computations given below, but then we have to introduce a different value of the true cohesion c.

We further assume that the volume of the sample remains constant during sampling and also during testing. The former assumption implies, firstly, that the capillary forces in the sample are sufficient to counteract the suction in the pore water, and secondly, that gases or any development of gases in the pore water do not occur. These assumptions may be correct for samples taken from a moderate depth, but they are certainly not correct for samples taken from a great depth. The latter assumption implies that the tests are made so rapidly that the escape of any pore water is completely prevented.

Finally, we assume the horizontal effective pressure in the ground to be equal to the earth pressure at rest, *i. e.*

$$\bar{\sigma}_h = K \bar{\sigma}_v$$

The shear strength of clays may be written

$$\tau = c + \bar{\sigma} \operatorname{tg} \varphi$$

where c is the true cohesion and $\bar{\sigma} \operatorname{tg} \varphi$ is the frictional component of the shear strength. We may confine ourselves to this expression. However, in some of the following computations we have deduced the expression for the true cohesion

$$c = c_0 + \varkappa \bar{\sigma}_{cm} \qquad \dots\dots\dots (1)$$

[1] The term origin cohesion denotes the cohesion (in this case = the shear strength) of normally consolidated (*i. e.* not preconsolidated) clay at the normal stress = 0. See (5).

where c_o is the origin cohesion and $\bar{\sigma}_{em}$ is the equivalent[1] average principal stress. In this case, when the clay is normally consolidated, the equivalent average principal stress is

$$\bar{\sigma}_{em} = \frac{1}{3}(\bar{\sigma}_v + 2\,\bar{\sigma}_h) = \frac{1}{3}\,\bar{\sigma}_v\,(1 + 2K)$$

Note. This hypothesis concerning the shear strength of clays differs from Hvorslev's well-known theory in two respects, *viz.*, first, as regards the constant c_o, *i. e.* the origin cohesion, which is not included in Hvorslev's theory, and may therefore be considered to be zero in his hypothesis, and second, as regards the increase of cohesion, $\frac{1}{3} \varkappa \bar{\sigma}_v (1 + 2K)$, which is here assumed to be proportional to the average principal stress, and not, as in Hvorslev's theory, proportional to the vertical (*i. e.* the major) principal stress (strictly speaking, to the vertical so-called equivalent stress, but, for normally consolidated clays, this is the same as the vertical effective stress). The reason for this departure from Hvorslev's theory is that all three principal effective stresses cause compression, and hence an increase of the cohesion (the Author assumes all these stresses to produce equal effects), and that some tests made by the Author (5) have shown that clay possesses so-called origin cohesion.

The hypothesis given here is somewhat suggestive of that due to Terzaghi (6)[2]

$$\tau = c_1 + \bar{\sigma} \operatorname{tg} \varphi_1 = c_1 + \frac{\bar{\sigma}_I + \bar{\sigma}_{III}}{2} \varkappa + \bar{\sigma} \operatorname{tg} \varphi$$

but the term c_1 comprises the origin cohesion as well as a part of the increase in cohesion due to consolidation by external forces. Furthermore, the influence of the mean principal stress is disregarded ($\bar{\sigma}_I$ is the major and $\bar{\sigma}_{III}$ is the minor effective principal stress).

The modulus of elasticity as well as Poisson's ratio vary during the shear tests when one of the effective principal stresses is increased and another is decreased, but we do not know exactly how they vary. In this analysis we therefore assume both the modulus of elasticity and Poisson's ratio to be constant. However, we use one value of the modulus of elasticity E_c corresponding to increasing pressure (compression) and another value E_s corresponding to decreasing pressure (swelling). According to Skempton (7), we denote the ratio of these values by $\frac{E_c}{E_s} = \lambda$. Furthermore, we use the symbol $\lambda_r = \frac{E_{cr}}{E_s}$ for the ratio of the values of the modulus of elasticity corresponding to recompression and to swelling.

The problem of determining the shear strength of anisotropically consolidated clay has been treated by Brinch Hansen and Gibson (8), and we shall deal with this problem the same way. However, in our case the expression for the shear strength is different (and so are the symbols). Moreover, there are some other differences. Brinch Hansen and Gibson have not compared the vane test and the unconfined compression test, and their expression for the unconfined com-

[1] The term "equivalent" has the same meaning as in Hvorslev's theory.

[2] We use slightly different notations, which agree with other symbols employed in this paper.

pression strength is not applicable in all cases. Besides, they have not treated the laboratory vane test.

In the computations we assume that the stresses are uniformly distributed over the surface of rupture. Thus we assume no degree of successive failure[1].

§ 8 b. Field Vane Test.

The surface of rupture is assumed to consist of a circular cylinder and two planes, so that all three of them taken together circumscribe the vane. This assumption is not quite self-evident, and cannot be correct in the boundaries between the vertical cylinder and the planes. But it seems to be an allowable approximation.

The shear strength τ_v computed from vane borings is an average shearing stress at failure across the whole surface of rupture.

$$\tau_v = \tau_{ver} \frac{1 + \frac{D}{3H} \cdot \frac{\tau_{hor}}{\tau_{ver}}}{1 + \frac{D}{3H}} \quad \ldots\ldots (2)$$

Thus we have to compute the shear strength τ_{ver} in a vertical surface of rupture and the shear strength τ_{hor} in a horizontal surface of rupture.

The vane was 65 mm in diameter and 130 mm in height. Hence $H = 2\,D$ and

$$\tau_v = \tau_{ver} \frac{6 + \frac{\tau_{hor}}{\tau_{ver}}}{7} \quad \ldots\ldots (3)$$

Shear Strength in Vertical Surface of Rupture.

At the beginning all horizontal effective normal stresses are $\bar{\sigma}_h = K\,\bar{\sigma}_v$. We may regard any two axes perpendicular to each other as principal axes. We choose those two axes which also remain principal at the end of the test.

At the end of the test one of the horizontal principal stresses has increased by, say, $\triangle\bar{\sigma}_1$ to $K\,\bar{\sigma}_v + \triangle\bar{\sigma}_1$, and the other horizontal principal stress has decreased by, say, $\triangle\bar{\sigma}_2$ to $K\,\bar{\sigma}_v - \triangle\bar{\sigma}_2$, while the vertical principal stress remains constant, provided there is no strain in this direction (7).

According to the λ-theory, we have

$$\triangle\bar{\sigma}_1 = \lambda\triangle\bar{\sigma}_2 \quad \ldots\ldots (4)$$

From the Mohr circle (Fig. 34) we get

$$\frac{\tau_{ver}}{\cos\varphi \sin\varphi} - \frac{c}{\operatorname{tg}\varphi} = K\,\bar{\sigma}_v + \frac{\triangle\bar{\sigma}_1 - \triangle\bar{\sigma}_2}{2} \quad \ldots\ldots (5)$$

and

$$\frac{\tau_{ver}}{\cos\varphi} = \frac{\triangle\bar{\sigma}_1 + \triangle\bar{\sigma}_2}{2} \quad \ldots\ldots (6)$$

[1] We use te expression "successive failure" for what is usually called "progressive failure".

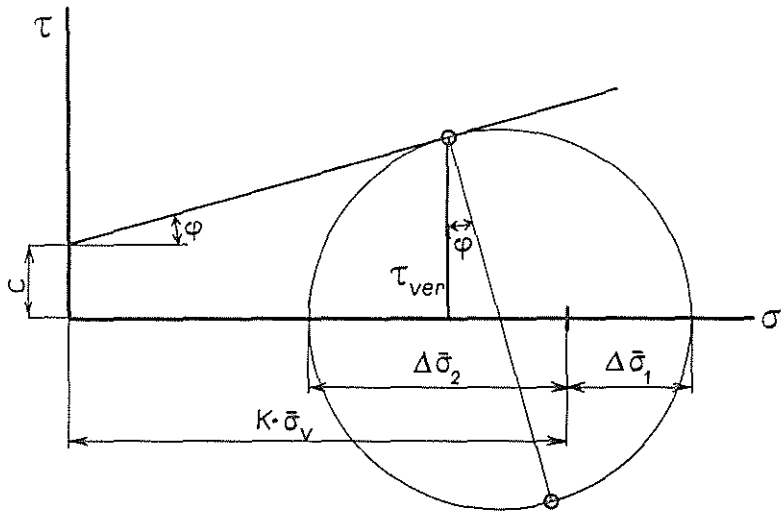

Fig. 34. Field vane test. Mohr's circle for determination of shear strength in vertical surface of rupture.

By eliminating $\triangle\bar{\sigma}_1$ and $\triangle\bar{\sigma}_2$ from Eqs. (4) to (6), we obtain

$$\tau_{ver} = \cos\varphi \frac{K\bar{\sigma}_v \sin\varphi + c \cos\varphi}{1 + n \sin\varphi} \quad \ldots\ldots\ldots\ldots\ldots\ldots\ldots\ldots\ldots\ldots \quad (7)$$

where

$$n = \frac{1-\lambda}{1+\lambda}$$

and

$$c = c_o + \frac{1}{3} \varkappa \bar{\sigma}_v \ (1 + 2\,K) \text{ according to Eq. (1).}$$

Shear Strength in Horizontal Surface of Rupture.

At the beginning one principal effective stress is vertical and equal to $\bar{\sigma}_v$, while the two others are horizontal and equal to $\bar{\sigma}_h = K\,\bar{\sigma}_v$ (Stage I, Fig. 35). As the moment on the vane increases, the principal axes turn. Since the surface of rupture is horizontal, the major principal stress at failure will make an angle of $45° - \frac{\varphi}{2}$ with the horizon (Stage II, Fig. 35). We assume that there is no strain in the (horizontal) radial direction during the test. This means that the principal stress in this direction remains unchanged (7). In order to be able to use the λ-method, we have to choose those axes (perpendicular to each other) along which the shearing stress remains constant during the test.[1]

[1] When the shearing stress is constant, it cannot have any influence on the water content of a volume element or, when the water content is constant, on the pore water pressure. Therefore, we have to consider the normal stresses only, just as in the case when the principal axes remain unchanged.

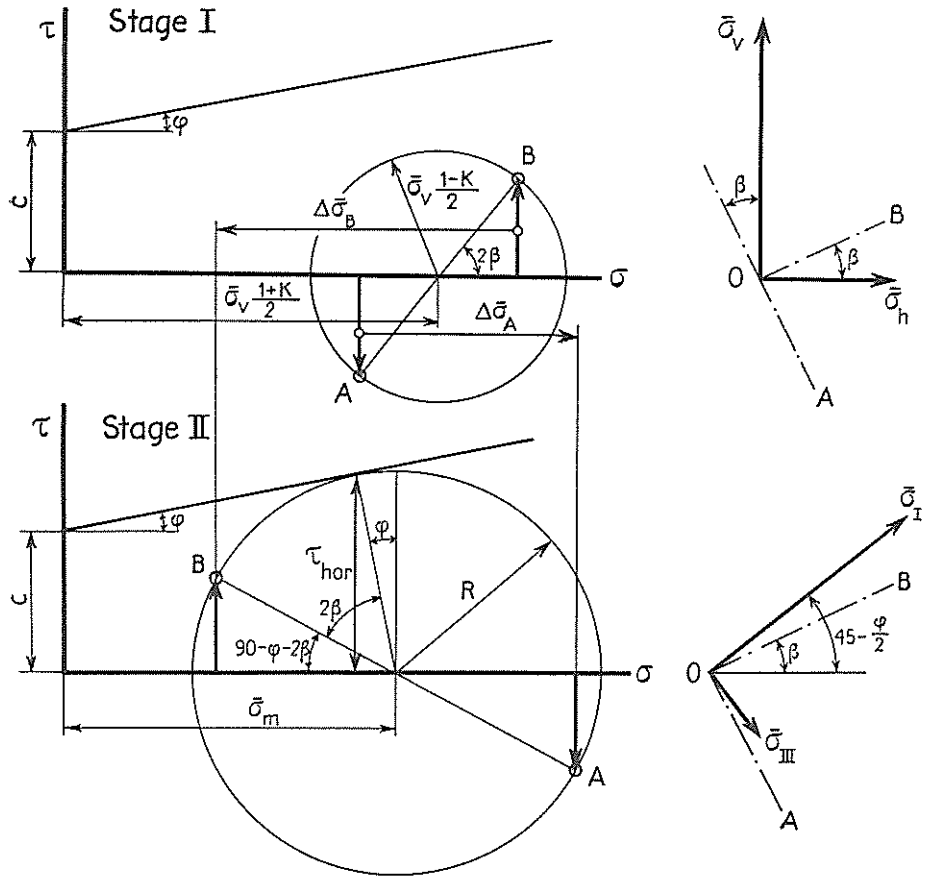

Fig. 35. Field vane test. Mohr's circle for determination of shear strength in horizontal surface of rupture.

Let β denote the angles these axes make with the horizon and the vertical, respectively, (Fig. 35). Then the above condition gives the equation

$$\bar{\sigma}_v \frac{1-K}{2} \sin 2\beta = R \sin (90 - \varphi - 2\beta) \quad \ldots\ldots\ldots\ldots\ldots\ldots \quad (8)$$

(The symbol R is explained in Fig. 35.)

By using the λ-method, which implies that the increase $\triangle\bar{\sigma}_A$ of the one normal stress shall be equal to λ times the decrease $\triangle\bar{\sigma}_B$ of the other normal stress, we get

$$\bar{\sigma}_m + R \cos (90 - \varphi - 2\beta) - \bar{\sigma}_v \frac{1+K}{2} + \bar{\sigma}_v \frac{1-K}{2} \cos 2\beta =$$

$$= \lambda \left[\bar{\sigma}_v \frac{1+K}{2} + \bar{\sigma}_v \frac{1-K}{2} \cos 2\beta - \bar{\sigma}_m + R \cos (90 - \varphi - 2\beta) \right] \quad (9)$$

(The symbol $\bar{\sigma}_m$ is explained in Fig. 35.)

Finally, the condition for rupture gives (Fig. 35)

$$\frac{R}{\sin\varphi} - \frac{c}{\operatorname{tg}\varphi} = \bar{\sigma}_m \quad \ldots\ldots\ldots\ldots\ldots\ldots\ldots\ldots\ldots\ldots\ldots\ldots\ldots\ldots\ldots\ldots \quad (10)$$

We eliminate β and $\bar{\sigma}_m$ from Eqs. (8) to (10) and solve them for R. Then we get the shear strength in the surface of rupture $\tau_{hor} = R \cos\varphi$.

This calculation gives

$$\tau_{hor} = \frac{\cos\varphi}{1 - n^2\sin^2\varphi}\left\{c\cos\varphi + \frac{1}{2}\bar{\sigma}_v \sin\varphi\,[1 + K + n^2\,(1 - K)\sin^2\varphi] \pm\right.$$

$$\pm n\sin\varphi\sqrt{c^2\cos^2\varphi + 2c\,\bar{\sigma}_v \sin\varphi\cos\varphi + \frac{\bar{\sigma}_v^2}{4}[(1-K)^2 +}$$

$$\left. + (1+K)\,(3-K)\sin^2\varphi - n^2\,(1-K)^2\sin^2\varphi\cos^2\varphi]\right\} \quad \ldots\ldots\ldots \quad (11)$$

The sign before the square root can be determined, for instance, by putting $K = 1$. Then Eqs. (7) and (11) should give the same value. This shows that the negative sign should be used.

From Eqs. (3), (7), and (11) we can now calculate the shear strength τ_v determined by our field vane test, when we know the values of

φ, K, $\bar{\sigma}_v$, λ, and c (or c_0 and $\varkappa$).

§ 8 c. Laboratory Vane Test.

In the ground, the effective vertical stress in the sample was equal to $\bar{\sigma}_v$ and the effective horizontal stress was $\bar{\sigma}_h = K\,\bar{\sigma}_v$. After extraction, the stresses in the sample are equal in all directions. The effective vertical stress has decreased by, say, $\Delta\bar{\sigma}_1$ and both effective horizontal stresses have increased by, say, $\Delta\bar{\sigma}_2$.

Then we have

$$2\,\Delta\bar{\sigma}_2 = \lambda\,\Delta\bar{\sigma}_1$$

$$\bar{\sigma}_v - \Delta\bar{\sigma}_1 = \bar{\sigma}_h + \Delta\bar{\sigma}_2$$

which gives

$$\Delta\bar{\sigma}_1 = \frac{\bar{\sigma}_v - \bar{\sigma}_h}{1 + \frac{\lambda}{2}} = \bar{\sigma}_v \frac{1 - K}{1 + \frac{\lambda}{2}}$$

and hence the effective stress $\bar{\sigma}_s$ in the three directions

$$\bar{\sigma}_s = \bar{\sigma}_v - \bar{\sigma}_v \frac{1 - K}{1 + \frac{\lambda}{2}} = \bar{\sigma}_v \frac{2K + \lambda}{2 + \lambda} \quad \ldots\ldots\ldots\ldots\ldots\ldots\ldots\ldots \quad (12)$$

The same expression has been deduced by Brinch Hansen and Gibson (8).

During the test the principal stresses change again.

Just as in the field vane test, the surface of rupture is assumed to consist of a circular cylinder and two end planes circumscribing the vane.

Shear Strength in Vertical Surface of Rupture.

We assume that the average of the two horizontal effective principal stresses (which are equal at the beginning of the test) decreases during the test by $\Delta\bar{\sigma}$ to

$$\bar{\sigma}_v \frac{2K+\lambda}{2+\lambda} - \Delta\bar{\sigma}$$

One of these stresses decreases from

$$\bar{\sigma}_v \frac{2K+\lambda}{2+\lambda}$$

to

$$(\bar{\sigma}_v \frac{2K+\lambda}{2+\lambda} - \Delta\bar{\sigma})\ (1-\sin\varphi) - c\cos\varphi \text{ (see Fig. 36)}$$

The other increases from

$$\bar{\sigma}_v \frac{2K+\lambda}{2+\lambda}$$

to

$$(\bar{\sigma}_v \frac{2K+\lambda}{2+\lambda} - \Delta\bar{\sigma})\ (1+\sin\varphi) + c\cos\varphi$$

Note: It is not self-evident that this principal stress should increase. However, it is easily shown that this will happen when $\lambda > 0$, which usually is the case.

The third principal stress (vertical) will remain unchanged (if there is no strain in this direction).

According to the λ-theory (increase in stress $= \lambda$ times decrease in stress), we get

$$\bar{\sigma}_v \frac{2K+\lambda}{2+\lambda}\sin\varphi - \Delta\bar{\sigma}\,(1-\sin\varphi) + c\cos\varphi =$$

$$= \lambda\left[\bar{\sigma}_v \frac{2K+\lambda}{2+\lambda}\sin\varphi + \Delta\bar{\sigma}\,(1-\sin\varphi) + c\cos\varphi\right]$$

which gives

$$\Delta\bar{\sigma} = \frac{\bar{\sigma}_v \frac{2K+\lambda}{2+\lambda}\sin\varphi + c\cos\varphi}{\frac{1+\lambda}{1-\lambda} + \sin\varphi}$$

and hence (from Mohr's circle, Fig. 36)

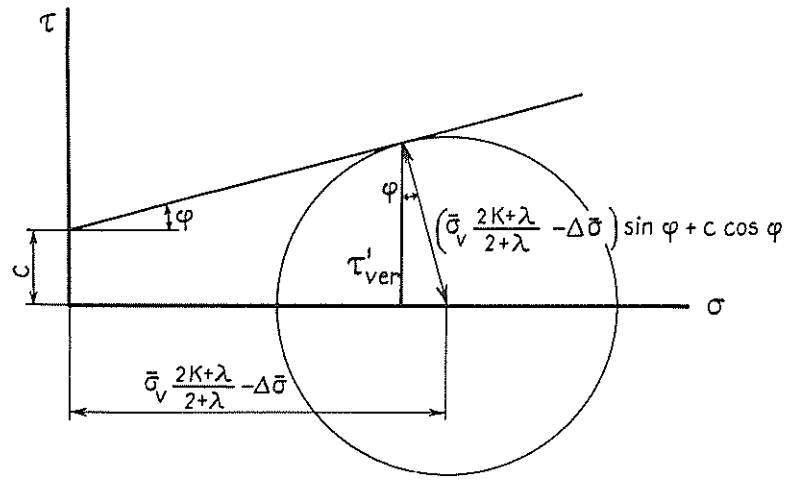

Fig. 36. Laboratory vane test. Mohr's circle for determination of shear stresses.

$$\tau'_{ver} = \left(\bar{\sigma}_v \frac{2K+\lambda}{2+\lambda} - \frac{\bar{\sigma}_v \frac{2K+\lambda}{2+\lambda} \sin\varphi + c\cos\varphi}{\frac{1+\lambda}{1-\lambda} + \sin\varphi} \right) \sin\varphi\cos\varphi + c\cos^2\varphi$$

or, after reduction,

$$\tau'_{ver} = \cos\varphi \frac{\bar{\sigma}_v \frac{2K+\lambda}{2+\lambda} \sin\varphi + c\cos\varphi}{1+n\sin\varphi} \quad \ldots\ldots\ldots\ldots\ldots\ldots \quad (13)$$

Shear Strength in Horizontal Surface of Rupture.

Just as in the field vane test, we assume the strain in the radial direction to be zero, so that the principal stress in this direction remains constant. Both other principal stresses are situated in a circular cylinder having the same axis as the vane. At the end of the test the major principal stress will make an angle of $(45° - \frac{\varphi}{2})$, and the minor principal stress will make an angle of $(45° + \frac{\varphi}{2})$, with the horizon (the surface of rupture). We choose these two directions for our computations. This is permissible as they are also principal at the beginning of the test.

We assume that the average of the major and the minor effective principal stress (which are equal at the beginning of the test) decreases during the test by $\Delta\bar{\sigma}$ to

$$\bar{\sigma}_v \frac{2K+\lambda}{2+\lambda} - \Delta\bar{\sigma}$$

At the end of the test the minor principal stress is (*cf.* Fig. 36)

$$(\bar{\sigma}_v \frac{2K+\lambda}{2+\lambda} - \triangle\bar{\sigma})\ (1 - \sin\varphi) - c\ \cos\varphi$$

and the major principal stress is

$$\bar{\sigma}_v\ \frac{2K+\lambda}{2+\lambda} - \triangle\bar{\sigma})\ (1 - \sin\varphi) + c\ \cos\varphi$$

Thus one principal stress has decreased during the test by

$$\triangle_d = \bar{\sigma}_v \frac{2K+\lambda}{2+\lambda} \sin\varphi + \triangle\bar{\sigma}\,(1 - \sin\varphi) + c\,\cos\varphi$$

The other has increased by

$$\triangle_i = \bar{\sigma}_v \frac{2K+\lambda}{2+\lambda} \sin\varphi - \triangle\bar{\sigma}\,(1 + \sin\varphi) + c\,\cos\varphi$$

Concerning this increase, we have to remember that the normal stress in the ground (that is, before sampling) in the direction of $\triangle_i$ was

$$\frac{\bar{\sigma}_v + \bar{\sigma}_h}{2} - \frac{\bar{\sigma}_v - \bar{\sigma}_h}{2} \cos\,(90° - \varphi) = \frac{\bar{\sigma}_v}{2}\,[1 + K - (1 - K)\,\sin\varphi]$$

This normal stress is practically always greater than the normal stress in the sample before the test. The corresponding condition is

$$\lambda < 2\,\frac{1 - \sin\varphi}{1 + \sin\varphi}$$

Thus the stress increase during the test implies recompression to the stress that existed in the ground.

The final value of the major principal stress after the test may be either greater or smaller than the stress in the ground. Accordingly, we have to distinguish between two cases A and B.

A. $\quad \frac{\bar{\sigma}_v}{2}[1 + K - (1 - K)\ \sin\ \varphi] < (\bar{\sigma}_v \frac{2K+\lambda}{2+\lambda} - \triangle\bar{\sigma})\ (1 + \sin\varphi) + c\ \cos\ \varphi$

The first step of the stress increase

$$\triangle_{i1} = \frac{\bar{\sigma}_v}{2}[1 + K - (1 - K)\ \sin\ \varphi] - \bar{\sigma}_v \frac{2K+\lambda}{2+\lambda}$$

is a recompression, whereas the second step

$$\triangle_{i2} = (\bar{\sigma}_v \frac{2K+\lambda}{2+\lambda} - \triangle\bar{\sigma})\ (1 + \sin\ \varphi) + c\ \cos\varphi - \frac{\bar{\sigma}_v}{2}[1 + K -$$
$$- (1 - K)\ \sin\varphi]$$

is a compression.

The λ-theory gives

$$\frac{\triangle_{i1}}{\lambda_r} + \frac{\triangle_{i2}}{\lambda} = \triangle_d$$

By inserting the expressions for $\triangle_{i1}$, $\triangle_{i2}$, and $\triangle_d$, and by solving the above equation for $\triangle\bar{\sigma}$, we get

$$\triangle\bar{\sigma} = \frac{\bar{\sigma}_v \left\{ \frac{2K+\lambda}{2+\lambda} [\lambda_r - \lambda + \lambda_r (1-\lambda) \sin\varphi] - \frac{\lambda_r - \lambda}{2} [1 + K - (1-K) \sin\varphi] \right\} + \lambda_r (1-\lambda) c \cos\varphi}{\lambda_r [1 + \lambda + (1-\lambda) \sin\varphi]} \quad \ldots\ldots\ldots\ldots\ldots\ldots \quad (14)$$

B. $\frac{\bar{\sigma}_v}{2} [1 + K - (1-K) \sin\varphi] > (\bar{\sigma}_v \frac{2K+\lambda}{2+\lambda} - \triangle\bar{\sigma}) (1 - \sin\varphi) + c \cos\varphi$

The whole step of stress increase is a recompression, and the λ-theory therefore yields

$$\bar{\sigma}_v \frac{2K+\lambda}{2+\lambda} \sin\varphi - \triangle\bar{\sigma} (1 + \sin\varphi) + c \cos\varphi = \lambda_r [\bar{\sigma}_v \frac{2K+\lambda}{2+\lambda} \sin\varphi + + \triangle\bar{\sigma} (1 - \sin\varphi) + c \cos\varphi]$$

The solution of this equation gives

$$\triangle\bar{\sigma} = \frac{1-\lambda_r}{1 + \lambda_r + (1-\lambda_r) \sin\varphi} (\bar{\sigma}_v \frac{2K+\lambda}{2+\lambda} \sin\varphi + c \cos\varphi) \ldots\ldots \quad (15)$$

When $\triangle\bar{\sigma}$ is determined by Eq. (14) or Eq. (15), we get (from Mohr's circle, Fig. 36)

$$\tau'_{hor} = \cos\varphi \left\{ (\bar{\sigma}_v \frac{2K+\lambda}{2+\lambda} - \triangle\bar{\sigma}) \sin\varphi + c \cos\varphi \right\} \ldots\ldots\ldots\ldots \quad (16)$$

Finally, we obtain from Eq. (2)

$$\tau'_v = \tau'_{ver} \frac{1 + \frac{D}{3H} \frac{\tau'_{hor}}{\tau'_{ver}}}{1 + \frac{D}{3H}} = \tau'_{ver} \frac{1 + \frac{15.3}{3 \cdot 30} \frac{\tau'_{hor}}{\tau'_{ver}}}{1 + \frac{15.3}{3 \cdot 30}} = \tau'_{ver} \frac{1 + 0.17 \frac{\tau'_{hor}}{\tau'_{ver}}}{1.17} \ldots \quad (17)$$

§ 8 d. Unconfined Compression Test.

At the beginning of the test all three effective principal stresses are equal, and are given by

$$\bar{\sigma}_v \frac{2K+\lambda}{2+\lambda} \text{ (see § 8 c)}$$

During the test the total vertical stress increases from zero to σ, while the total horizontal stresses remain zero. The effective vertical stress increases by, say, $\triangle\bar{\sigma}_1$ and each of the effective horizontal stresses decreases by, say, $\triangle\bar{\sigma}_2$.

We now have to distinguish between two cases A and B.

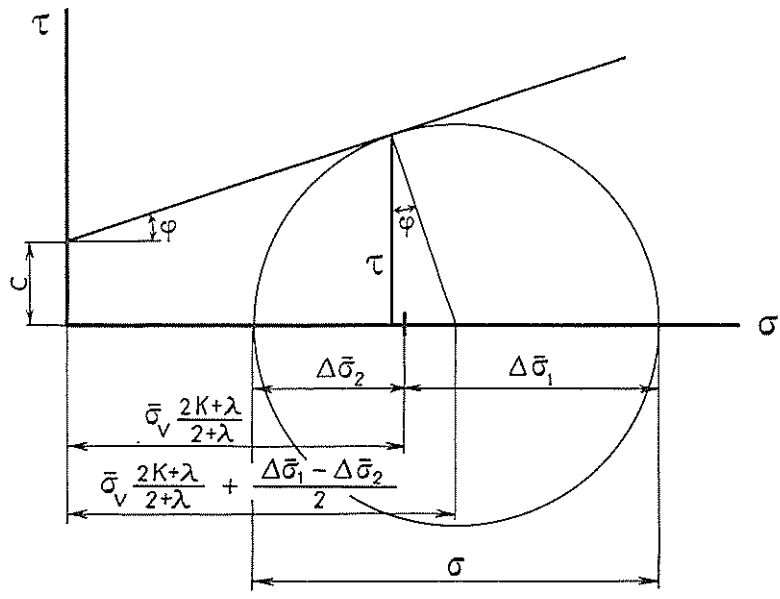

Fig. 37. Unconfined compression test. Mohr's circle for determination of shear stresses.

A. $$\bar{\sigma}_v > \bar{\sigma}_v \frac{2K+\lambda}{2+\lambda} + \Delta\bar{\sigma}_1$$

The increase of the vertical effective stress from

$$\bar{\sigma}_v \frac{2K+\lambda}{2+\lambda} \text{ to } \bar{\sigma}_v \frac{2K+\lambda}{2+\lambda} + \Delta\bar{\sigma}_1$$

implies recompression, and we have to use the recompressibility ratio λ_r. As the volume of the sample remains constant during the test, we have

$$\Delta\bar{\sigma}_1 = 2\,\lambda_r\,\Delta\bar{\sigma}_2$$

From Mohr's circle we get (Fig. 37)

$$\left[\bar{\sigma}_v \frac{2K+\lambda}{2+\lambda} + \frac{\Delta\bar{\sigma}_1}{2} - \frac{\Delta\bar{\sigma}_2}{2} + \frac{c}{\operatorname{tg}\varphi}\right] \sin\varphi = \frac{\Delta\bar{\sigma}_1}{2} + \frac{\Delta\bar{\sigma}_2}{2}$$

Inserting

$$\Delta\bar{\sigma}_2 = \frac{1}{2\,\lambda_r}\,\Delta\bar{\sigma}_1$$

we obtain

$$\Delta\bar{\sigma}_1 = 2\,\frac{\bar{\sigma}_v \frac{2K+\lambda}{2+\lambda}\sin\varphi + c\cos\varphi}{1 + \frac{1}{2\,\lambda_r} - \sin\varphi\left(1 - \frac{1}{2\,\lambda_r}\right)}$$

Now,

$$\tau_c = \frac{\sigma}{2} = \frac{\triangle \bar{\sigma}_1}{2}\left(1 + \frac{1}{2\,\lambda_r}\right)$$

and hence

$$\tau_c = \frac{1 + 2\,\lambda_r}{1 + \sin\varphi + 2\,\lambda_r\,(1 - \sin\varphi)}\left(c\cos\varphi + \bar{\sigma}_v\,\frac{2K + \lambda}{2 + \lambda}\sin\varphi\right) \ldots \quad (18)$$

The same expression has been deduced by Brinch Hansen and Gibson.

However, they have not treated Case B.

B. $\qquad \bar{\sigma}_v < \bar{\sigma}_v \frac{2K + \lambda}{2 + \lambda} + \triangle \bar{\sigma}_1$

The increase of the vertical effective stress from $\bar{\sigma}_v \frac{2K + \lambda}{2 + \lambda}$ to $\bar{\sigma}_v$ implies recompression, and for this increase we have to use the recompressibility ratio λ_r, while the increase from $\bar{\sigma}_v$ to $\bar{\sigma}_v \frac{2K + \lambda}{2 + \lambda} + \triangle \bar{\sigma}_1$, implies compression, and for this increase we have to use the compressibility ratio λ.

Thus we get

$$\frac{1}{\lambda_r}\left(\bar{\sigma}_v - \bar{\sigma}_v \frac{2K + \lambda}{2 + \lambda}\right) + \frac{1}{\lambda}\left(\bar{\sigma}_v \frac{2K + \lambda}{2 + \lambda} + \triangle \bar{\sigma}_1 - \bar{\sigma}_v\right) = 2\,\triangle \bar{\sigma}_2$$

From Mohr's circle we get as before

$$\left(\bar{\sigma}_v \frac{2K + \lambda}{2 + \lambda} + \frac{\triangle \bar{\sigma}_1}{2} - \frac{\triangle \bar{\sigma}_2}{2} + \frac{c}{\operatorname{tg}\varphi}\right)\sin\varphi = \frac{\triangle \bar{\sigma}_1}{2} + \frac{\triangle \bar{\sigma}_2}{2}$$

By solving these two equations for $\triangle \bar{\sigma}_1$ and $\triangle \bar{\sigma}_2$, we obtain

$$\tau_c = \frac{\triangle \bar{\sigma}_1}{2} + \frac{\triangle \bar{\sigma}_2}{2}$$

This calculation gives

$$\tau_c = \frac{\bar{\sigma}_v\left[\frac{2K + \lambda}{2 + \lambda}\left(2\,\lambda + \frac{\lambda}{\lambda_r}\right) + 1 - \frac{\lambda}{\lambda_r}\right]\sin\varphi + c\;(1 + 2\,\lambda)\;\cos\varphi}{1 + \sin\varphi + 2\,\lambda\;(1 - \sin\varphi)} \quad . \quad (19)$$

§ 8 e. Numerical Values.

The test results given in § 6 are expressed in terms of the ratio of the shear strength determined by the unconfined compression test and the laboratory vane test to the shear strength determined by the field vane test. The theoretical results obtained in this section will be expressed in the same way.

First, we have to assume certain values of the characteristics of the clay, that is, values of

φ, K, λ, λ_r, c_o, and z

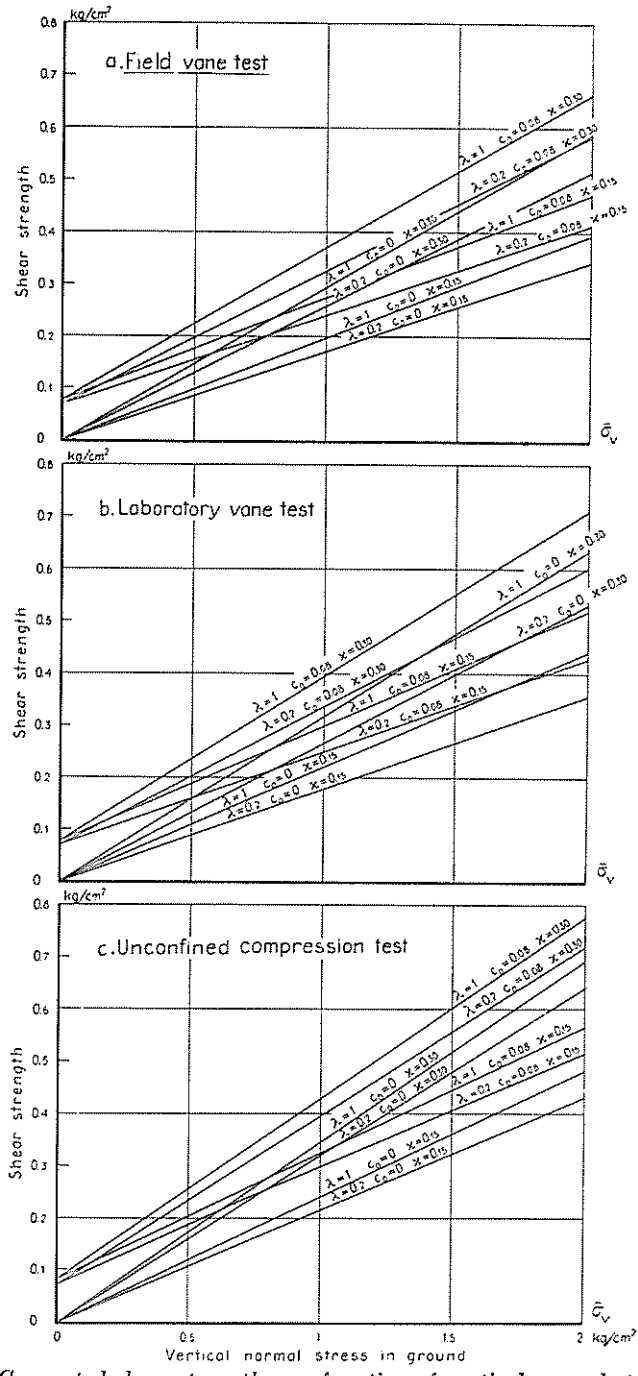

Fig. 38. Computed shear strength as a function of vertical normal stress in the ground. (Assumptions: the clay is normally consolidated, the angle of internal friction is 11°, and the recompressibility ratio is equal to unity.)

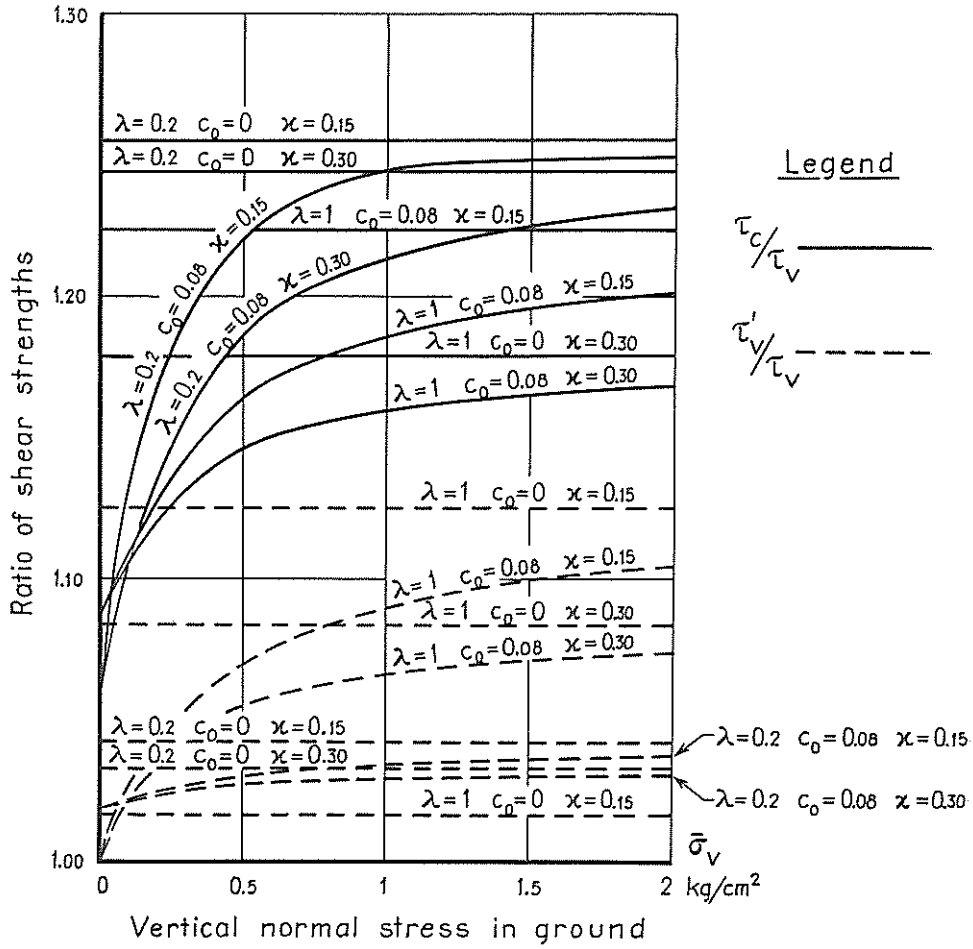

Fig. 39. Computed ratios of shear strengths (unconfined compression test and laboratory vane test) to strength obtained from field vane test as functions of vertical normal stress in ground. (Assumptions: the clay is normally consolidated, the angle of internal friction is 11°, and the recompressibility ratio is equal to unity.)

For the true angle of internal friction, φ, we choose the value 11° taken from earlier investigations of Swedish clays (9).

For the coefficient K of earth pressure at rest we have found the value 0.5 for a Swedish clay (test made with undisturbed sample). This is in good agreement with the values given by Tschebotarioff (10).

The coefficient λ is assumed to be equal to 0.2 according to the consolidation tests involving the removal of load mentioned in § 6. However, we have also chosen the value $\lambda = 1$, which implies that the clay strictly obeys Hooke's law

(equal values of the modulus of elasticity for application and removal of load). The coefficient λ_r is supposed to be equal to 1 according to consolidation tests involving the removal and the reapplication of load mentioned in § 6.

The origin cohesion c_o is assumed to be 0.08 kg/cm^2 according to earlier investigations (5). However, we have also assumed the value $c_o = 0$, which implies that the clay strictly follows Hvorslev's theory in this respect.

Finally, the coefficient of increase in cohesion $\varkappa$ normally varies from 0.15 to 0.30 [when the true cohesion is expressed by Eq. (1)]. These two values of $\varkappa$ have been assumed.

By using the above values, and Eqs. (3), (7), and (11), we obtain the shear strength determined by the field vane test as a function of the normal vertical effective pressure in the ground, see Fig. 38 a.

By using the above values and Eqs. (14), (15), (16), and (17), we obtain the shear strength determined by the laboratory vane test as a function of the normal vertical effective pressure in the ground, see Fig. 38 b.

By using the above values and Eqs. (18) and (19), we obtain the shear strength determined by the unconfined compression test as a function of the normal vertical effective pressure in the ground, see Fig. 38 c.

Finally, we have computed the ratio of the shear strength determined by the unconfined compression test and the laboratory vane test to the shear strength determined by the field vane test, see Fig. 39.

There is an obvious difference in Fig. 39 between the curves computed on the basis of a certain definite value of the origin cohesion and on the curves computed without taking account of the origin cohesion. The latter show a constant ratio of the values of the shear strength determined by means of different methods, while the former show a ratio increasing with the normal stress. Figs. 22 to 30 should therefore indicate whether there is any origin cohesion in the ground in this case. However, because of the scattering of the curves, we cannot discern any clear trend.

Figs. 38 and 39 also show the influence of the coefficient λ. When λ increases from 0.2 to 1, all values of the shear strength increase. The values obtained from the laboratory vane test increase most, while the values obtained from the unconfined compression test (Fig. 38) increase least, but the difference is not very great. Thus the ratio of the values obtained from the unconfined compression test to those obtained from the field vane test decreases, while the ratio of the values obtained from the laboratory vane test to those obtained from the field vane test increases (except the values corresponding to a very small normal stress), (Fig. 39).

§ 9. Discussion of Test Results and Conclusions.

§ 9 a. Influence of Sampler Type.

Figs. 22 to 30 show that there is a great difference between the shear strengths of samples taken by means of samplers of different types. This difference must be due to variations of the samplers in respect of area ratio, range, edge angle, shutter, and so on. Of course, the best way to investigate the effects of these factors would have been to vary each of them separately, while keeping all the others constant. This was not possible, but we can nevertheless draw some conclusions from the tests.

An extremely small area ratio offers no special advantages (for instance, compare Fig. 25 with Fig. 22 or 28). Thus samplers with tight-fitting piston and open samplers (which were investigated by Hvorslev) behave quite differently.

The edge angle in our types of samplers does not seem to have any great influence. However, an extremely great area ratio or edge angle is not recommendable (compare Fig. 23 with Fig. 22).

An increase of the range increases the strength of the samples (compare Fig. 26 and Fig. 22), but this increase is not great so long as the samples are kept in the liners, *i. e.* in the cone test and in the laboratory vane test.

The highest values of the shear strength were obtained on samples taken with the pneumatic piston sampler (Fig. 28). The most important difference between this type of sampler and the others lies in the velocity and the continuity of release of the drive during sampling. It is therefore evident that this drive should be rapid and continuous, as has already been mentioned by Hvorslev.

From Fig. 28 we see that, for depths smaller than 13 m, the values given by the unconfined compression test are about 15 % greater, the values obtained from the laboratory vane test are about 10 % smaller, than those resulting from field vane test. According to our theoretical computations, the unconfined compression test should give values which are about 20 % greater, and the laboratory vane test should give values which are about 5 % greater, than those obtained from field vane test. Considering that the values of the shear strength according to the unconfined compression test in Figs. 22 to 30 are slightly too great (see p. 21), we can state that even the best type of sampler causes a decrease of about 10 % in the shear strength of samples taken from moderate depths. For samples taken from comparatively great depths, the decrease in strength is greater, at least in the unconfined compression test. The difference between the values obtained from the unconfined compression test and the laboratory vane test is in good agreement with the theoretical computations for samples taken from depths down to 13 m.

It is interesting to compare the pneumatic sampler with shutter (Fig. 28) and that without shutter (Fig. 27). The curves relating to the two bore holes where the former was used agree very well (Fig. 31). The curves corresponding to the two holes where the latter was used agree partly with each other and

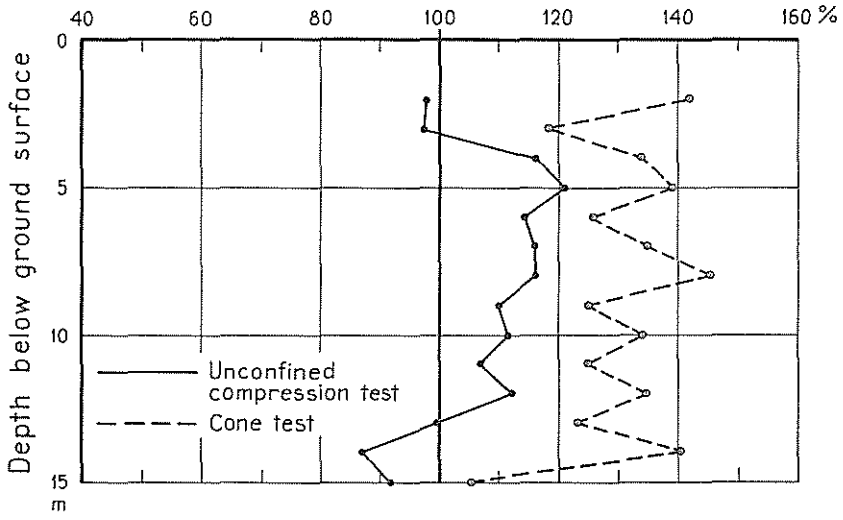

Fig. 40. Ratio of shear strength of unpunched samples taken by means of sampler with metal foils to strength obtained from field vane test.

with the curves just mentioned, but include some extremely low values (Fig. 32). It is quite evident that these values of the shear strength represent disturbed samples. At these points the sampling failed, and afterwards, during withdrawal, the empty sampler sucked in disturbed soil from a higher level. Some special experiments have shown that this is quite possible. Thus our experience concerning the pneumatic sampler indicates that when we really extract a sample from a correct level, the shutter has no influence on the shear strength of the sample. But the shutter is necessary in order to ensure correct operation of the sampler.

In § 6 is stated that, in cutting out samples of our normal diameter from the cores (taken by means of the sampler with metal foils), the punch had an influence on the shear strength. We can say that punching has the same effect as new sampling, and hence causes a new slight disturbance of the clay. An investigation of unpunched samples, *i. e.* samples having the same diameter as the core, was made down to a depth of 15 m below ground surface (Fig. 40). On these samples we made only unconfined compression tests and cone tests. Although the outermost part of the samples (of the core) may be disturbed by the foils, the values obtained from the unconfined compression test on the unpunched samples were higher than those relating to the punched samples (compare Figs. 40 and 30). In the cone test, however, just the contrary was the case. One reason of this may be that only the punched samples, and not the unpunched samples, were laterally confined during the cone test. Another explanation is that the end surfaces of the unpunched samples were somewhat disturbed when the samples were cut from the core, since the wire saw was not guided.

§ 9 b. Influence of Testing Method.

For samples taken from depths down to about 15 m, the cone test gives the greatest value of the shear strength, then comes the unconfined compression test, while the laboratory vane test gives the lowest values. Type *a* and *b* samplers are exceptions in this respect.

For samples taken from depths greater than 15 m, the order of tests arranged according to decreasing shear strength values is as follows: cone test, laboratory vane test, and unconfined compression test, but the difference between the two latter tests is very slight for several types of samplers. An explanation of this circumstance is given below.

During sampling, the samples lose some of their shear strength, partly owing to the disturbance caused by the sampler, partly owing to a decrease in total stress, which causes a decrease in the sum of the effective principal stresses. The latter decrease may be due to the unsufficient capillarity of the clay or to the presence or development of gases in the pore water. Some decrease, although probably very little, is also due to the fact that the sample must undergo a slight swelling in order to cause the formation of menisci in the pore water, and thus to enable suction in the pore water. Finally, the change in stresses causes a decrease in the sum of the effective principal stresses for all values of $\lambda < 1$ (and $K < 1$). The decrease in strength caused by the change in stress will occur even if the sampler is quite perfect, and the amount of this decrease with the depth from which the sample is taken. In other words, the loss of shear strength will increase with the depth.

However, it seems that this loss is not very great so long as the samples are enclosed in their liners. Therefore, it appears that a certain loss occurs when the samples are pushed out of the liners. Now we have to remember that there is a difference between the unconfined compression test on one hand, and the laboratory vane test and the cone test on the other hand (at least as the tests have been made here). While the specimen in the unconfined compression test is of course entirely unconfined, it is completely confined in the vane test, and it may be said to be partly confined in the cone test (since this test is made on an end plane of the specimen kept in the liner). Consequently, if the results of the unconfined compression test, the laboratory vane test, and the cone test are expressed in terms of their respective ratios to the results of the field vane test, then the decrease in these ratios with depth should be greatest for the unconfined compression test and smallest for the laboratory vane test, as is in fact shown by our results (Figs. 22 to 30).

In our above discussion we have assumed that there is no disturbance during the field vane test. Of course, this cannot be quite true, but we believe that the error may be neglected in this connection.

At first sight it may seem strange that, for some types of samplers, the unconfined compression test gives higher values than the field vane test when the samples are taken from depths smaller than about 15 m. This was the

reason why we made our theoretical analysis, see § 8. As may be seen from Fig. 39, it is quite natural that both the unconfined compression test and the laboratory vane test should give higher values than the field vane test, provided that the sample is quite undisturbed. The magnitude of the difference between these values is dependent on the characteristics of the clay.

The values of the shear strength of the samples obtained from the cone test are evidently too high. However, we have to distinguish between the shear strength of the samples and the shear strength of the soil. We are most interested in the latter, but we try to determine it by testing samples. The cone test was calibrated long ago, mainly by comparison with the strength of the soil computed from slides. The test was then made on samples taken with a sampler similar to Type *h*, which disturbs the samples considerably. It is evident that the cone test gives a reliable value of the shear strength of the ground when use is made of a Type *h* or Type *d* sampler. On one hand, the values of the shear strength of the samples obtained from the cone test are too high. On the other hand, the samplers disturb the samples in some way or other. For the above-mentioned two types of samplers, these two factors compensate each other. But it is not certain, and not even probable, that this is the case in all kinds of clays, since the cone factor (the bearing capacity factor) is certainly variable.

Bibliography.

1. Kjellman, W., Kallstenius, T. & Wager, O., Soil Sampler with Metal Foils. Stockholm 1950. (R. Swed. Geot. Inst. Proc. Nr 1.)
2. Hvorslev, M. Juul, Subsurface Exploration and Sampling of Soils. New York 1949.
3. Lambe, T. W., Soil Testing for Engineers. New York and London 1951. p. 117.
4. Terzaghi, K., Undisturbed Clay Samples and Undisturbed Clays. J. Boston Soc. Civ. Engrs. 1941 Vol. 28 Nr 3 p. 211—231.
5. Jakobson, B., Origin Cohesion of Clay. Proc. 3. internat. Conf. Soil Mech. a. Found. Engng. 1953 Vol. 1 p. 35—37.
6. Terzaghi, K., Theoretical Soil Mechanics. New York 1944. p. 9.
7. Skempton, A. W., The Effective Stresses in Saturated Clays Strained at Constant Volume. Proc. 7. internat. Congr. appl. Mech. 1948.
8. Brinch Hansen, J. & Gibson, R. E., Undrained Shear Strengths of Anisotropically Consolidated Clays. Géotechnique 1949 Vol. 1 Nr 3 p. 189—204.
9. Jakobson, B., The Landslide at Surte on the Göta River. Stockholm 1952. (R. Swed. Geot. Inst. Proc. Nr 5.)
10. Tschebotarioff, G., Discussion of paper Vc 3. Proc. 2. internat. Conf. Soil Mech. a. Found. Engng. 1948 Vol. 6 p. 108—111.